SIAM J. CONTROL OPTIM.
Vol. 55, No. 3, pp. 1347–1376

SHAPE OPTIMIZATION OF SHELL STRUCTURE ACOUSTICS*

HARBIR ANTIL†, SEAN HARDESTY‡, AND MATTHIAS HEINKENSCHLOSS§

Abstract. This paper provides a rigorous framework for the numerical solution of shape optimization problems in shell structure acoustics using a reference-domain approach. The structure is modeled with Naghdi shell equations, fully coupled to boundary integral equations on a minimally regular surface, permitting the formulation of three-dimensional radiation and scattering problems on a two-dimensional set of reference coordinates. We prove well-posedness of this model, and Fréchet differentiability of the state with respect to the surface shape. For a class of shape optimization problems we prove existence of optimal solutions under slightly stronger surface regularity assumptions. Finally, adjoint equations are used to efficiently compute derivatives of the radiated field with respect to large numbers of shape parameters, which allows consideration of a rich space of shapes and, thus, of a broad range of design problems. A numerical example is presented to illustrate the applicability of our theoretical results.

Key words. structural acoustics, Naghdi shell, boundary integral equation, shape derivative, shape optimization

AMS subject classifications. 74K25, 65R20, 35Q93, 49Q10

DOI. 10.1137/16M1070633

1. Introduction.

We propose and analyze a mathematical model for shape optimization of shell structure acoustics. The structure is modeled with Naghdi shell equations and is fully coupled to boundary integral equations for the acoustics. This allows the formulation of three-dimensional radiation and scattering problems on a two-dimensional set of reference coordinates. While components of our coupled system of shell equations and boundary integral equations have been discussed in the literature, the coupled problem and shape optimization governed by this coupled system is new. We establish well-posedness of the coupled shell and boundary integral equation. The shape optimization problem is formulated using a reference-domain framework in which the shape is parametrized by a midsurface chart function and a thickness function. The shape optimization problem thus becomes a nonlinear PDE-constrained optimal control problem. We prove existence of optimal solutions under slightly stronger surface regularity assumptions than are needed for the well-posedness of the governing coupled system. Possible existence of so-called Jones modes requires us to add norm constraints on the states to ensure existence of optimal solutions. In addition, we prove Fréchet differentiability of the state with respect to the midsurface chart and thickness functions and use the adjoint equation approach to compute the derivative of the objective function with respect to the parameterization of the shell. Due to the specific objective function in our application, the adjoint equation approach is slightly nonstandard and care must be taken in how it is applied. We will

*Received by the editors April 15, 2016; accepted for publication (in revised form) January 5, 2017; published electronically May 2, 2017.

http://www.siam.org/journals/sicon/55-3/M107063.html

Funding: The work of SH and MH has been supported in part by NSF VIGRE grant DMS-0739420, NSF grants DMS-0915238, DMS-1115345, and AFOSR grant FA9550-12-1-0155. The work of HA has been partially supported by NSF grant DMS-1521590.

†Department of Mathematical Sciences, George Mason University, Fairfax, VA 22030 (hantil@gmu.edu).

‡Z-Terra Inc., 17171 Park Row, Ste. 247, Houston, TX 77084 (hardesty@z-terra.com).

§Department of Computational and Applied Mathematics, MS-134, Rice University, Houston, TX 77005-1892 (heinken@rice.edu).

first illustrate the issue on a simple example and then formulate the adjoint equation approach for our application. A numerical example is presented to demonstrate the applicability of our theory.

Shell structures are ubiquitous in nature because they are light but strong: roughly speaking, their geometry allows loads to be balanced by tensile strains rather than by bending. Engineers use them in a wide variety of applications. Some of these serve an acoustic function, e.g., loudspeakers [17] and musical instruments [60, 30]. Although other examples, such as automobiles [44, 46], must primarily suit mechanical objectives, their acoustic behavior is also an important design consideration. The development of computer modeling and optimization tools is important for the design of shell structures, and this paper provides a theoretical foundation for such tools.

In the frequency domain, the governing equations for the displacement $\widetilde{u} : \widetilde{\Omega} \subset \mathbb{R}^3 \to \mathbb{C}^3$ and the velocity potential $\varphi : \mathbb{R}^3 \setminus \widetilde{\Omega} \to \mathbb{C}$ are given by the linear elasticity equation coupled with the Helmholtz equation. This coupling makes $\widetilde{u}$ complex-valued; as with the Helmholtz equation, the physical quantity is simply the real part. In the following, $c > 0$ is the speed of sound in the acoustic medium, $\rho_0 > 0$ is the density of the air, $\rho : \widetilde{\Omega} \to \mathbb{R}^+$ is the density of the elastic material, $H : \widetilde{\Omega} \to \mathbb{R}^{3\times3\times3\times3}$ is the constitutive tensor, f is a boundary traction, and $e(\widetilde{u}) = \frac{1}{2}(\nabla\widetilde{u} + (\nabla\widetilde{u})^T)$ is the strain tensor. For a given angular frequency $\omega = c\kappa$, the coupled problem is

$$-\omega^2\rho\widetilde{u}(\widetilde{x}) = \nabla \cdot \sigma(\widetilde{u}(\widetilde{x})), \qquad \widetilde{x} \in \widetilde{\Omega}, \tag{1a}$$

$$\sigma(\widetilde{u}(\widetilde{x})) = H : e(\widetilde{u}(\widetilde{x})), \qquad \widetilde{x} \in \widetilde{\Omega}, \tag{1b}$$

$$\sigma(\widetilde{u}(\widetilde{x})) \cdot n = f - i\omega\rho_0\varphi(\widetilde{x})n(\widetilde{x}), \qquad \widetilde{x} \in \partial\widetilde{\Omega}, \tag{1c}$$

$$\partial_n\varphi(\widetilde{x}) = -i\omega\widetilde{u}(\widetilde{x}) \cdot n(\widetilde{x}), \qquad \widetilde{x} \in \partial\widetilde{\Omega}, \tag{1d}$$

$$\Delta\varphi(\widetilde{x}) + \kappa^2\varphi(\widetilde{x}) = 0, \qquad \widetilde{x} \in \mathbb{R}^3 \setminus \widetilde{\Omega}, \tag{1e}$$

$$\left|\nabla\varphi \cdot \widetilde{x}/|\widetilde{x}| - i\kappa\varphi\right| = O\left(1/|\widetilde{x}|^2\right), \qquad \text{as } |\widetilde{x}| \to \infty. \tag{1f}$$

We consider "thin" domains $\widetilde{\Omega}$, i.e., those that can be parameterized by their midsurface and thickness. This representation of thin domains as well as kinematic assumptions on the displacement u are used to approximate the equations (1) by a system of equations on a reference domain Ω_0. Specifically, we replace the three-dimensional (3d) elasticity equations (1a)–(1c) by the 2d Naghdi shell equation, and we replace the Helmholtz equation (1d)–(1f) by a suitable "screen" boundary integral equation.

The Naghdi shell equations reduce the computational domain from three dimensions to two, at the cost of including somewhat rough geometric coefficient functions that encode the geometry of the shell midsurface. Finite element methods based on the Naghdi equations are in common use in engineering practice for calculations involving shell structures, although the implementation must deal appropriately with the so-called "locking" phenomenon; see [3, 42, 16]. Naghdi shell equations reduce further to the well-known Reissner–Mindlin plate model if the shell midsurface is flat.

Boundary integral equations are well suited to solving acoustic radiation and scattering problems in infinite domains because they automatically produce solutions satisfying the Sommerfeld radiation condition, without the need for artificial truncation of the exterior domain, and lend themselves to point measurement of the external field via a representation formula [54].

Trouble can ensue when typical boundary element methods are applied to thin structures: a shell will have approximately the same velocity normal to the midsurface

on either side, so that the pressure difference across the thin dimension is the relevant physical quantity. For very thin structures, failure to consider the thin dimension carefully can lead to instability. Helmholtz "screen" problems were thoroughly analyzed by Stephan in [58], and their derivation based on geometric approximations involved in translating the equations to the midsurface was done by Martinez in [49]. Our model uses this screen boundary integral formulation, which involves the jumps across the midsurface rather than separate values on either side.

Boundary integral equations coupled with plate models were used by Mariem and Hamdi [48], and later, by Gaul and Fischer [27], whose implementation deals with such issues as coupling of different mesh scales, acceleration of the BEM, and preconditioning of the resulting linear systems. Coupling of shell models with BEM was done in the context of shape optimization by Marburg et al. in [45, 47], [44, 46], [28]. However, none of these papers address basic questions of existence and uniqueness of solutions to the coupled problem: in particular, when driven in isolation, and in the absence of ad hoc viscous-type damping terms, uniqueness will fail at eigenfrequencies of the shell. For the coupled problem to have a unique solution, the acoustic radiation must damp these eigenmodes. This paper resolves this issue by proving a well-posedness result for the fully coupled system consisting of the Naghdi shell equations and screen boundary integral equations, including a characterization of the conditions under which uniqueness to the coupled problem can fail. We assume the midsurface to be only W^2_∞, the minimal possible regularity for the Naghdi shell problem to make sense; see [12, 14].

Numerical optimization of shell structure acoustics is performed in the papers [18, 45, 47, 44, 46]. However, none of these papers analyzes the underlying infinite-dimensional optimization approach or provides an adjoint equation approach for derivative computations. The paper [18] approximates derivatives using finite differences, [45, 47, 44, 46] use an approximate "semi-analytic" method, and [28] apply a sensitivity approach which requires the solution of a linear system for each shape parameter. These papers also drop the influence of the acoustic load on the structure, and assume that the motion of the shell structure can be expanded in a basis of eigenmodes, which is reasonable provided that the density of the acoustic medium is small compared to that of the structure, or that the optimization deals only with a few low frequencies. None of them use adjoint equations, hence they can handle only rather small shape parameter sets.

Adjoint equations are used by Sigmund et al. in [61] for topology optimization of a fluid-acoustics problem. But their approach is so expensive that it is done only in two spatial dimensions, and with a bounded domain. Adjoint equations are also employed in [41, 39], but in the absence of full coupling between the shells and the acoustic medium; their numerical examples only include very few shape parameters.

Sokołowski and Khludnev [38, 55] use the shape calculus presented, e.g., in [56] to compute shape derivatives for optimization problems governed by a Koiter thin shell. This shape calculus does not require a parametrization of the domain. No numerical results are given in [38, 55]. Instead, we formulate the shape optimization problem using a reference-domain framework in which the shape is parameterized by the midsurface chart function and the thickness function. As we have mentioned before, with our formulation the shape optimization problem becomes a nonlinear PDE-constrained optimal control problem, and optimization algorithms developed for optimal control problems are directly applicable. Since the mathematical model of thin shells already uses the midsurface chart and the thickness function, this approach of transforming to a reference domain seems particularly suitable for our application.

In section 5 we apply our approach to the shape optimization of shell structure acoustics for joined shells to show its utility.

This paper is organized as follows. In sections 2.1 and 2.2 we review the Naghdi shell equations and the screen boundary integral equations. Coupling of these equations and the analysis of the coupled system are performed in sections 2.3. Fréchet differentiability of the shell and boundary integral operators is established in sections 3 for W^2_∞ midsurfaces. A class of optimization problems is formulated and analyzed in section 4. In particular, we prove existence of optimal solutions for a standard class of objective functions, assuming a W^3_p midsurface, where $p > 2$. When Jones modes exist, the unique solution of the coupled shell acoustic system is not guaranteed. This difficulty is avoided by adding norm constraints on the state. Our analysis extends the results for the shell shape optimization problem studied in [2], which does not include coupling to the Helmholtz equation, uses a class of C^2 midsurfaces, and assumes compactness of the constraint set. In addition we compute derivatives of the objective function with respect to shape parameters using the adjoint equation approach and illustrate subtle issues that arise from the fact that the displacement and pressure are complex-valued functions. We conclude with a numerical example in sections 5.

2. The Model for the shell structure acoustic interaction. In this section, we review the derivation of the 2d Naghdi shell equations, which approximate the 3d elasticity equations (1a)–(1c), and of the "screen" boundary integral equation approximating the Helmholtz equation (1d)–(1f). Coupling them leads to a new model problem analogous to (1). We prove its well-posedness under suitable assumptions. Due to page limitations we have moved proofs and some technical details into a Supplement [1].

For definitions and properties of Sobolev and other function spaces we refer to the books by Hsiao and Wendland [35], McLean [50], and Sauter and Schwab [54]. Define

$$H^1_{\mathrm{loc}}(\Omega) := \left\{ u \in H^1(K) : \text{ for every compact set } K \subset \Omega \right\}.$$

The space $H^1_{\mathrm{loc}}(\Omega)$ can also be characterized by the statement [35, p. 192]

$$u \in H^1_{\mathrm{loc}}(\Omega) \text{ if and only if } \varrho u \in H^1(\Omega) \text{ for every } \varrho \in C^\infty_0(\mathbb{R}^n).$$

Throughout this paper $|\cdot|$ denotes the 2-norm of a real vector or matrix, or the modulus of a complex number. The notation $\|\cdot\|$ is used for function space norms (with subscript to indicate the corresponding function space).

2.1. Naghdi shells. When an elastic body is much smaller in one dimension than in the other two, it can be modeled using shell equations. The Naghdi shell model is derived from standard linear elasticity, reducing the original problem (1a)–(1c) from three dimensions to two. The classical derivation uses a kinematic assumption and a mechanical assumption, which are not strictly necessary: Delfour has developed a version of the Naghdi model based on "intrinsic" differential calculus, which avoids recourse to these assumptions [21, 22]. We follow the more classical approach proposed by Blouza and Le Dret [12, 14] because it is well known and closely tied to the implementation of the long-used mixed interpolated tensorial components (MITC) finite element methods; see [16, section 6.3], [15, 16].

In the derivation of Naghdi's model, we assume u to be real-valued. It will become complex-valued in section 2.3, when we couple it with the Helmholtz equation.

We consider "thin" domains, which are described by a so-called middle surface chart $\phi : \Omega_0 \subset \mathbb{R}^2 \to \mathbb{R}^3$ defined on a reference domain $\Omega_0 \subset \mathbb{R}^2$ and a thickness function $t : \Omega_0 \to \mathbb{R}^+$. We make the following assumptions.

(A1) The reference domain $\Omega_0 \subset \mathbb{R}^2$ is bounded and satisfies the strong local Lipschitz condition.

(A2) The chart function ϕ belongs to the set

$$\mathcal{C} = \Big\{ \phi \in W^2_\infty(\Omega_0)^3 : \phi \text{ is one-to-one and } \partial_\alpha \phi(x_1, x_2),\ \alpha = 1, 2, \text{are linearly independent for all } (x_1, x_2) \in \Omega_0 \Big\}. \tag{2}$$

We define the covariant basis vectors

$$a_\alpha(x_1, x_2) = \partial_\alpha \phi(x_1, x_2),\ \alpha = 1, 2, \tag{3a}$$

which span the plane tangent to the middle surface, and we define the unit normal to the middle surface

$$a_3(x_1, x_2) = \frac{a_1(x_1, x_2) \times a_2(x_1, x_2)}{|a_1(x_1, x_2) \times a_2(x_1, x_2)|}. \tag{3b}$$

The dual contravariant basis vectors a^i are defined via

$$a^i(x_1, x_2) \cdot a_j(x_1, x_2) = \delta^i_j,\ i, j = 1, 2, 3$$

where δ^i_j is the Kronecker delta. The covariant and contravariant components of the metric tensor are respectively

$$a_{ij} = a_i \cdot a_j, \quad (a^{ij}) = (a_{ij})^{-1}.$$

Furthermore we define the change of metric factor

$$\sqrt{a(x_1, x_2)} = \sqrt{a_{11}(x_1, x_2) a_{22}(x_1, x_2) - a_{12}(x_1, x_2)^2}. \tag{3c}$$

See [19, 16, 31] for more details on shell geometries.

Our domain is the image of the reference domain

$$\Omega = \Big\{ (x_1, x_2, x_3) \in \mathbb{R}^3 : (x_1, x_2) \in \Omega_0 \text{ and } |x_3| < t(x_1, x_2)/2 \Big\}, \tag{4}$$

under the mapping

$$\Phi(x_1, x_2, x_3) = \phi(x_1, x_2) + x_3 a_3(x_1, x_2) \tag{5}$$

(see Figure 1), and is given by

$$\widetilde{\Omega} = \Phi(\Omega).$$

For the remainder of this subsection we denote points in $\widetilde{\Omega}$ by $\widetilde{x}$ and points in Ω_0 by x. Greek subscripts and superscripts take values in $\{1, 2\}$, while Latin subscripts and superscripts take values in $\{1, 2, 3\}$. Throughout the paper we use the Einstein summation convention.

PROPOSITION 2.1. *If (A1) and (A2) hold, then the map $\Phi : \Omega_0 \times \mathbb{R} \to \mathbb{R}^3$ defined in (5) is a local W^1_∞-diffeomorphism.*

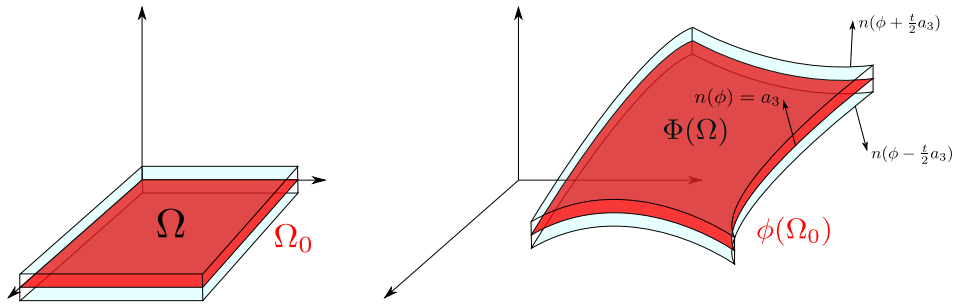

FIG. 1. *Naghdi shell geometry: The physical domain* $\widetilde{\Omega} = \Phi(\Omega)$ *is constructed via the thickness function* t *and the chart function* ϕ *through the mapping* $\Phi(x_1, x_2, x_3) = \phi(x_1, x_2) + x_3 a_3(x_1, x_2)$. *of the reference domain* $\Omega = \{(x_1, x_2, x_3) \in \mathbb{R}^3 : (x_1, x_2) \in \Omega_0 \text{ and } |x_3| < t(x_1, x_2)/2\}$.

Proof. See the Supplement [1]. ∎

We represent displacements on the reference domain Ω. For $\widetilde{x} = \Phi(x)$ we define

$$u(x) = \widetilde{u}(\Phi(x)) = \widetilde{u}(\widetilde{x}). \tag{6}$$

The Naghdi model of Blouza and Le Dret [12, 14] is derived from 3d elasticity on Ω by use of the Reissner–Mindlin kinematic assumption, i.e., by assuming the following form for the 3d elastic displacement:

$$u(x_1, x_2, x_3) = z(x_1, x_2) + x_3\theta(x_1, x_2). \tag{7}$$

The displacement $u : \Omega \to \mathbb{R}^3$ is composed of the displacement $z : \Omega_0 \to \mathbb{R}^3$ of the middle surface plus a first-order rotation $\theta : \Omega_0 \to \mathbb{R}^3$, with $\theta \cdot a_3 = 0$. This means that material lines normal to the undeformed middle surface can translate and make a first-order rotation.

To derive the Naghdi shell equations, the functions z and θ can be represented in the locally varying basis $\{a_1, a_2, a_3\}$ or the through their Cartesian components. To distinguish between between vectors and their components we temporarily use vector symbols. That is, we write

$$\vec{u}(x_1, x_2, x_3) = \vec{z}(x_1, x_2) + x_3\vec{\theta}(x_1, x_2)$$

instead of (7). To derive the Naghdi shell equations, the locally varying basis $\{\vec{a}_1, \vec{a}_2, \vec{a}_3\}$ is used to represent the shell geometry and the constitutive tensors. In the classical formulation (see, e.g., [16, section 4.2.2]) it is also used to represent $\vec{z}$ and $\vec{\theta}$: they are identified with their covariant components $z = (z_1, z_2, z_3)$ and $\theta = (\theta_1, \theta_2)$ via

$$\vec{z}(x_1, x_2) = z_i(x_1, x_2)\vec{a}^i(x_1, x_2), \quad \vec{\theta}(x_1, x_2) = \theta_\alpha(x_1, x_2)\vec{a}^\alpha(x_1, x_2).$$

Blouza and Le Dret [12, 14] instead represent the vectors appearing in (7) through their Cartesian components; in this vein, see also the more specialized papers by Le Dret [25], Sprekels and Tiba [57], and Bletzinger et al. [11]. The presentation in [12, 14] is simpler than the classical one and does not require differential geometry concepts such as covariant derivatives and the second fundamental form.

We adopt a hybrid approach in that we identify $\vec{\theta}$ with its covariant components and $\vec{z}$ with its Cartesian components; i.e., we drop the vector symbols and simply

write $\theta = (\theta_1, \theta_2)$ to indicate the covariant components of $\vec{\theta}$, and $z = (z_1, z_2, z_3)$ to indicate the Cartesian components of $\vec{z}$. Thus, the kinematic assumption appears:

$$u(x_1, x_2, x_3) = z(x_1, x_2) + x_3\theta_\alpha(x_1, x_2)a^\alpha(x_1, x_2). \tag{8}$$

This choice will allow us to formulate the problem in a function space that does not depend on ϕ as does that of Blouza and Le Dret through the tangency condition $\vec{\theta} \cdot \vec{a}_3 = 0$, and in fact is more closely tied to practical finite element implementation than either the classical approach or that of Blouza and Le Dret [12, 14]; see [16, section 6.3].

If we use the geometric assumptions on $\widetilde{\Omega} = \Phi(\Omega)$ stated above, (6), as well as the kinematic assumption (8) for u and a corresponding assumption $v(x_1, x_2, x_3) = y(x_1, x_2) + x_3\eta_\alpha(x_1, x_2)a^\alpha(x_1, x_2)$ for the test function, the 3d elastic bilinear form

$$\int_{\widetilde{\Omega}} (H : e(\widetilde{u})(\widetilde{x})) : e(\widetilde{v})(\widetilde{x})\, d\widetilde{x}$$

leads to

$$\begin{aligned} K(\theta, z; \eta, y) := \int_{\Omega_0} \Bigg(& C^{\alpha\beta\lambda\mu}\left[t\gamma_{\alpha\beta}(z)\gamma_{\lambda\mu}(y) + \frac{t^3}{12}\chi_{\alpha\beta}(\theta, z)\chi_{\lambda\mu}(\eta, y)\right] \\ & + tD^{\lambda\mu}\zeta_\lambda(\theta, z)\zeta_\mu(\eta, y)\Bigg)\sqrt{a(x)}\, dx. \end{aligned} \tag{9}$$

Here the Naghdi constitutive tensors $C^{\alpha\beta\lambda\mu}$ and $D^{\lambda\mu}$ are obtained from the constitutive tensor H in (1b). The tensors γ, χ, ζ, which correspond to membrane stretching, bending, and transverse shear, respectively, are given by

$$\gamma_{\alpha\beta}(z) \stackrel{\text{def}}{=} \tfrac{1}{2}\big(a_\alpha(x) \cdot \partial_\beta z(x) + a_\beta(x) \cdot \partial_\alpha z(x)\big), \tag{10a}$$

$$\begin{aligned} \chi_{\alpha\beta}(\theta, z) \stackrel{\text{def}}{=} \tfrac{1}{2}\big(& a_\alpha(x) \cdot \partial_\beta(\theta_\lambda(x)a^\lambda(x)) + a_\beta(x) \cdot \partial_\alpha(\theta_\lambda(x)a^\lambda(x)) \\ & + \partial_\alpha a_3(x) \cdot \partial_\beta z(x) + \partial_\beta a_3(x) \cdot \partial_\alpha z(x)\big), \end{aligned} \tag{10b}$$

$$\zeta_\alpha(\theta, z) \stackrel{\text{def}}{=} \tfrac{1}{2}\big(\theta_\alpha(x) + a_3(x) \cdot \partial_\alpha z(x)\big). \tag{10c}$$

The form of these tensors is as in Blouza and Le Dret [12, 14], in contrast to the classical formulation, which makes use of covariant derivatives and the second fundamental form. Using covariant derivatives here would simplify the appearance of the terms in χ involving θ, but would obscure the dependence on the chart function ϕ. We note that these tensors still make sense for charts that are W^2_∞: the classical formulation required a C^3 chart in order to formulate the standard problem of a shell clamped on an edge because the Koiter rigid-body lemma was not known until [13, Thm. 6] to hold for W^2_∞ charts. In our problem, derived from (1), no clamping is applied, and the rigid-body lemma is not required.

Similarly, applying the geometry description and the Naghdi assumption (8) to

$$\int_{\widetilde{\Omega}} \rho\widetilde{u}(\widetilde{x}) \cdot \widetilde{v}(\widetilde{x})\, d\widetilde{x},$$

which corresponds to the weak form of the left-hand side in (1a), leads to the Naghdi inertial form

$$M(\theta, z; \eta, y) := \int_{\Omega_0} \rho\left(tz(x) \cdot y(x) + \frac{t^3}{12}\theta_\alpha(x)a^{\alpha\beta}\eta_\beta(x)\right)\sqrt{a(x)}\, dx. \tag{11}$$

The (weak form of the) equations (1a–1c) are replaced by the following Naghdi shell equations. Let

$$\mathcal{S} = H^1(\Omega_0)^2 \times H^1(\Omega_0)^3. \tag{12}$$

We seek $(\theta, z) \in \mathcal{S}$ such that

$$K(\theta, z; \eta, y) - \omega^2 M(\theta, z; \eta, y) = \int_{\Omega_0} h(x) \cdot y(x) \sqrt{a(x)}\, dx \tag{13}$$

for all $(\eta, y) \in \mathcal{S}$. Here h is determined from the right-hand side (1c).

We make the following assumptions on the Naghdi constitutive tensors.

(A3) There exist constants $0 < c_1 < c_2$ and $0 < c_3 < c_4$ such that for almost all $x \in \Omega_0$ and all symmetric tensors γ, χ and all vectors ζ, ξ,

$$C^{\alpha\beta\lambda\mu}(x)\gamma_{\alpha\beta}\gamma_{\lambda\mu} \geq c_1 \sum_{\alpha,\beta} \gamma_{\alpha\beta}^2, \qquad C^{\alpha\beta\lambda\mu}(x)\gamma_{\alpha\beta}\chi_{\lambda\mu} \leq c_2 \gamma_{\alpha\beta}\chi_{\alpha\beta},$$
$$D^{\lambda\mu}(x)\zeta_\lambda\zeta_\mu \geq c_3 \sum_{\lambda} \zeta_\lambda^2, \qquad D^{\lambda\mu}(x)\zeta_\lambda\xi_\mu \leq c_4 \zeta_\lambda\xi_\lambda.$$

Blouza and LeDret [14, Lemma 3.6] use assumptions (A2) and (A3) to prove that the bilinear form K in (9) is bounded and coercive on $\mathcal{S}_0 \times \mathcal{S}_0$ provided that the shell is clamped and $\mathcal{S}_0 \subset \mathcal{S}$ is the subspace that incorporates the clamping condition. To analyze the coupled problem we will need a slightly different result.

We first make the following standard assumption for the thickness function t.

(A4) The thickness function t belongs to the set

$$\mathcal{T} = \left\{ t \in L^\infty(\Omega_0) : t(x) \geq t_{\min} > 0 \text{ for almost all } x \in \Omega_0 \right\}. \tag{14}$$

LEMMA 2.2. *If the assumptions* (A1)–(A4) *hold, there exists a constant* $k_0 > 0$ *such that the bilinear form*

$$((\theta, z), (\eta, y)) \mapsto K(\theta, z; \eta, y) + k_0 \int_{\Omega_0} \theta(x) \cdot \eta(x) + z(x) \cdot y(x)\, dx$$

on $\mathcal{S} \times \mathcal{S}$ *is bounded and coercive.*

Proof. See the Supplement [1]. ∎

Remark 2.3. In the next section, and for the rest of the paper, the field variables (θ, z) are assumed to be complex-valued, with the real part being the physical value. For a complex-valued forcing function h, the analogue to (13) is

$$K(\theta, z; \overline{\eta}, \overline{y}) - \omega^2 M(\theta, z; \overline{\eta}, \overline{y}) = \int_{\Omega_0} h(x) \cdot \overline{y}(x) dx. \tag{15}$$

In particular h depends on φ and is used to couple (15) with the approximation of the Helmholtz equation (1d)–(1f).

Since K (9) and M (11) are real, symmetric bilinear forms, Lemma 2.2 remains valid if complex-valued (θ, z) and $(\overline{\eta}, \overline{y})$ are used.

In the next subsection we describe the approximation of the Helmholtz equation (1d)–(1f), and then we state and analyze the coupled system, which contains (15).

2.2. Screen boundary integral equations. We continue to use the geometry description of the shell introduced in the previous section. In this section we discuss the approximation of the Helmholtz equation (1d)–(1f) by a boundary integral equation on the midsurface $\phi(\Omega_0)$ of the shell. This leads to the so-called "screen" problem studied by Stephan [58]. In this section we outline the approximations that lead to the screen problem, sketch the derivation of the corresponding boundary integral equations, and summarize results that will be needed to state and analyze the coupled problem.

To arrive at the screen problem we consider the Helmholtz equation (1d)–(1f) and make the following approximations; see Martinez [49].

(S1) The surfaces $\{\phi(x) \pm t(x)a_3(x)/2 : x \in \Omega_0\}$ of the shell (see Figure 1) are approximated by the middle surface $\phi(\Omega_0)$.

(S2) The normals on the shell surfaces $\{\phi(x) \pm t(x)a_3(x)/2 : x \in \Omega_0\}$ are approximated using the midsurface normal $n(\phi(x)) = a_3(x)$.

We emphasize the physical nature of the approximations (S1), (S2): if the thickness of the shell is small compared to acoustic wavelengths, it is reasonable to pose the problem as if the acoustic coupling actually happens on the middle surface. The thickness function t retains a strong influence over the way in which the shell moves, but has no direct effect on the acoustic coupling. Due to the smoothness assumption (A2) on the chart function ϕ, the midsurface normal $n(\phi(x)) = a_3(x)$ is well defined. The Reissner–Mindlin kinematic assumption (8) assures that the normal velocity $u \cdot n$ is the same on both sides of the shell and is given by $z \cdot n$, and therefore the Helmholtz screen equation with Neumann data can be coupled with the Naghdi model in a kinematically consistent way.

With the approximations (S1), (S2), the Helmholtz equation (1d)–(1f) on the exterior of the shell $\widetilde{\Omega} = \Phi(\Omega)$ can be approximated by the following equation on the exterior of the midsurface $\phi(\Omega_0)$ of the shell. To simplify the notation, we denote the midsurface by

$$\Gamma_0 \stackrel{\text{def}}{=} \phi(\Omega_0). \tag{16}$$

The approximation of (1d)–(1f) is given by

$$\Delta\varphi(\widetilde{x}) + \kappa^2\varphi(\widetilde{x}) = 0, \qquad \widetilde{x} \in \mathbb{R}^3 \setminus \Gamma_0, \tag{17a}$$

$$\partial_n\varphi(\widetilde{x}) = g(\widetilde{x}), \qquad \widetilde{x} \in \Gamma_0, \tag{17b}$$

$$\left|\nabla\varphi \cdot \widetilde{x}/|\widetilde{x}| - i\kappa\varphi\right| = O\left(1/|\widetilde{x}|^2\right), \qquad \text{as } |\widetilde{x}| \to \infty. \tag{17c}$$

The right-hand side g in (17b) is derived from the right-hand side in (1d). Let $\widetilde{x} = \phi(x)$ and let $x \in \Omega_0$ be a point on the midsurface Γ_0. If we use (6), (8) and (S1), (S2), then the right-hand side $-i\omega\widetilde{u}(\widetilde{x}) \cdot n(\widetilde{x})$ in (1d) corresponds to

$$g(\phi(x)) = -i\omega z(x) \cdot n(\phi(x)) = -i\omega z(x) \cdot a_3(x). \tag{18}$$

where $\phi(x)$, $x \in \Omega_0$, is a point on the midsurface Γ_0.

Next, we recall the uniqueness result for the screen problem (17); the existence result will be provided in Theorem 2.6, following from the equivalence between the screen problem and a corresponding boundary integral equation, established in Lemma 2.5.

LEMMA 2.4. *Let* (A1) *and* (A2) *hold. If* $\varphi \in \{\varrho \in H^1_{loc}(\mathbb{R}^3 \setminus \Gamma_0) : (\Delta + \kappa^2)\varrho = 0$ *in* $\mathbb{R}^3 \setminus \Gamma_0$ *and* ϱ *satisfies* (17c)$\}$ *solves* (17) *with* $g = 0$*, then* $\varphi = 0$.

Proof. See [58, Lemma 2.1] and [31, Lemma 4.3.5]. ∎

We equivalently reformulate (17) as a boundary integral equation. The Green's function for the Helmholtz equation is

$$G(\widetilde{x},\widetilde{x}') = \frac{\exp(i\kappa|\widetilde{x}'-\widetilde{x}|)}{4\pi|\widetilde{x}'-\widetilde{x}|}.$$

We extend the shell midsurface Γ_0 to a Lipschitz continuous surface $\Gamma \supset \Gamma_0$ such that Γ is the boundary of a bounded Lipschitz domain $G_1 \subset \mathbb{R}^3$. Thus,

$$\Gamma_0 \subset \Gamma = \partial G_1. \tag{19}$$

We denote by γ^- and γ^+ respectively the trace operator from the interior and exterior of G_1, and by ∂_n^- and ∂_n^+ respectively the interior and exterior normal derivative on ∂G_1. The jump in φ on the shell midsurface Γ_0 is denoted by

$$[\varphi] \stackrel{\text{def}}{=} \gamma^+\varphi - \gamma^-\varphi. \tag{20}$$

The solution φ to the screen problem (17) is given by the representation formula (see the Supplement [1] or [58])

$$\varphi(\widetilde{x}') = \int_{\Gamma_0} [\varphi](\widetilde{x})\, \partial_{n,\widetilde{x}} G(\widetilde{x},\widetilde{x}')\, d\widetilde{x} \quad \text{for } \widetilde{x}' \notin \Gamma_0. \tag{21}$$

Since we are given Neumann boundary data in (17), we take the normal derivative of (21) to derive an integral equation for the jump of φ across the shell midsurface Γ_0.

To derive the boundary integral operator corresponding to the screen problem, we first review the hypersingular operator corresponding to the Helmholtz equation for $\Gamma = \partial G_1$. The double-layer potential DL applied to $\varsigma \in L^1(\Gamma)$ is

$$\big(DL\varsigma\big)(\widetilde{x}') = \int_\Gamma \partial^+_{n,\widetilde{x}} G(\widetilde{x},\widetilde{x}')\varsigma(\widetilde{x})\, d\widetilde{x},$$

see, e.g., [20], and the hypersingular integral operator is defined by

$$D \stackrel{\text{def}}{=} -\partial_n^{\pm} DL : H^{1/2}(\Gamma) \to H^{-1/2}(\Gamma).$$

The representation of $\langle D\varphi, \varrho\rangle_{H^{-1/2}(\Gamma)\times H^{1/2}(\Gamma)}$ can be found, e.g., in [50, Thm. 9.15] and is given by the right-hand side in (23b) below with Γ_0 replaced by Γ.

The restriction of D to the surface patch $\Gamma_0 = \phi(\Omega_0)$ is denoted D_{Γ_0}. It is shown in [58, Lemma 2.2] that the proper space for the jump $[\varphi]$ is

$$\widetilde{H}^{1/2}(\Gamma_0) = \left\{ u \in H^{1/2}(\Gamma) : \operatorname{supp}(u) \subset \overline{\Gamma}_0 \right\}. \tag{22}$$

The physical significance of this is that the pressure jump at the edge is zero. We define

$$D_{\Gamma_0} : \widetilde{H}^{1/2}(\Gamma_0) \to H^{-1/2}(\Gamma_0) \tag{23a}$$

with

$$\begin{aligned}\langle D_{\Gamma_0}[\varphi], \varrho\rangle_{H^{-1/2}(\Gamma_0)\times \widetilde{H}^{1/2}(\Gamma_0)} &= \iint_{\Gamma_0} G(\widetilde{x},\widetilde{x}')(n_{\widetilde{x}} \times \nabla[\varphi]) \cdot (n_{\widetilde{x}'} \times \nabla \varrho)\, d\widetilde{x} d\widetilde{x}' \\ &\quad - \kappa^2 \iint_{\Gamma_0} G(\widetilde{x},\widetilde{x}')([\varphi] n_{\widetilde{x}}) \cdot (\varrho n_{\widetilde{x}'})\, d\widetilde{x} d\widetilde{x}'.\end{aligned} \tag{23b}$$

The next lemma establishes the equivalence between the differential equation (17) and the integral equation (24) below. As mentioned before, the idea behind (24) is taking the normal derivative of (21) and replacing the resulting left-hand side $\partial_n \varphi$ on the shell midsurface Γ_0 be the boundary data g.

LEMMA 2.5. *Assume that* (A1) *and* (A2) *hold and let the Neumann data* $g \in H^{-1/2}(\Gamma_0)$ *be given. The function* $\varphi \in H^1_{loc}(\mathbb{R}^3 \setminus \Gamma_0)$ *solves* (17) *if and only if its jump* $[\varphi] \in \widetilde{H}^{1/2}(\Gamma_0)$ *solves the integral equation*

$$D_{\Gamma_0}[\varphi] = -g. \tag{24}$$

Proof. This result was shown for smooth surfaces in [58, Theorem 2.6] but can be easily extended to Lipschitz surfaces using the ideas from Costabel [20]. ∎

Because the Naghdi chart function ϕ determines the geometry for both the shell and boundary integral equations, we formulate (24) on the reference domain Ω_0.

Let $\Omega_0 \subset \mathbb{R}^2$, with the chart function $\phi \in \mathcal{C} \subset W^2_\infty(\Omega_0)^3$. The weak form to be evaluated for the hypersingular operator D is (23). In order to transform this integral over $\Gamma_0 = \phi(\Omega_0)$ into an integral over Ω_0, the quantities a_3 and $\sqrt{a}$, defined in (3), are needed. Through transformation of the integral over $\Gamma_0 = \phi(\Omega_0)$ into an integral over Ω_0, the product $\langle D_{\Gamma_0}[\varphi], \varrho \rangle_{H^{-1/2}(\phi(\Omega_0)) \times \widetilde{H}^{1/2}(\phi(\Omega_0))}$ becomes

$$\begin{aligned}\langle D(\phi)\psi, \varrho\rangle_{\Omega_0} = &\iint_{\Omega_0} G(\phi(x), \phi(x'))\,(a_3(x') \times \nabla\Phi^{-T}(x')\widetilde{\nabla}\psi(x'))\\ &\times (a_3(x) \times \nabla\Phi^{-T}(x)\widetilde{\nabla}\varrho(x))\sqrt{a(x')a(x)}\,dx'dx\\ &- \kappa^2 \iint_{\Omega_0} G(\phi(x), \phi(x'))\,(a_3(x')\psi(x')) \cdot (a_3(x)\varrho(x))\sqrt{a(x')a(x)}\,dx'dx,\end{aligned} \tag{25}$$

where Φ is defined in (5) and the derivative $\widetilde{\nabla}$ is defined via

$$\widetilde{\nabla}\rho(x) = \begin{pmatrix}\partial_{x_1}\rho(x) & \partial_{x_2}\rho(x) & 0\end{pmatrix}^T.$$

In (25) the notation $D(\phi)$ is used to emphasize that for the screen $\phi(\Omega_0)$ the hypersingular operator depends on the chart function ϕ. We use $\psi \in \widetilde{H}^{1/2}(\Omega_0)$ for the jump in the velocity potential defined in the reference domain.

THEOREM 2.6. *Assume that* (A1) *and* (A2) *hold and let the Neumann data* $g \in H^{-1/2}(\Gamma_0)$ *be given. There exists a unique solution* $\psi \in \widetilde{H}^{1/2}(\Omega_0)$ *to*

$$\langle D(\phi)\psi, \varrho\rangle_{H^{-1/2}(\Omega_0) \times \widetilde{H}^{1/2}(\Omega_0)} = -\langle g \circ \phi, \varrho\rangle_{H^{-1/2}(\Omega_0), \widetilde{H}^{1/2}(\Omega_0)} \quad \forall \varrho \in \widetilde{H}^{1/2}(\Omega_0), \tag{26}$$

where $D(\phi)$ *is as given in* (25). *In addition, the solution depends continuously on the data* g, *i.e., there exists a constant* $c > 0$ *such that*

$$\|\psi\|_{\widetilde{H}^{1/2}(\Omega_0)} \le c\|g \circ \phi\|_{H^{-1/2}(\Omega_0)}.$$

Proof. See the Supplement [1]. ∎

2.3. The coupled shell and boundary integral equations. We couple the models from section 2.1 and section 2.2 and prove existence and uniqueness of the solution. Recall that $\phi \in \mathcal{C} \subset W^2_\infty(\Omega_0)^3$ is the chart function representing the midsurface

$$\Gamma_0 = \phi(\Omega_0)$$

of the shell. For the rest of the paper, all function spaces are taken to be over $\mathbb{C}$, including $\mathcal{S}$, defined in (12). The physical midsurface displacement z, rotation angle θ, and velocity potential φ are simply the real parts of these complex-valued functions.

In the following, x denotes a point in Ω_0 and $\widetilde{x}$ denotes a point in $\mathbb{R}^3 \setminus \Gamma_0$ or on Γ_0. The functions $\theta, z, \eta, y, f, \rho$ are defined on the reference domain Ω_0, while the velocity potential φ and the normal n are defined respectively on $\mathbb{R}^3 \setminus \Gamma_0$ and on Γ_0. Therefore, the argument of n is $\phi(x)$ if, for example, we integrate over Ω_0. For $\widetilde{x} \in \Gamma_0 = \phi(\Omega_0)$ we often write $z(x) \cdot n(\widetilde{x})$. In this case the argument $x \in \Omega_0$ of z is the point in the reference domain Ω_0 such that $\widetilde{x} = \phi(x)$.

First, we combine the Naghdi shell equations from section 2.1 with the screen problem (17) to approximate (1). We seek $(\theta, z) \in \mathcal{S}$, where $\mathcal{S}$ is defined in (12), and φ in $H^1_{\mathrm{loc}}(\mathbb{R}^3 \setminus \phi(\Omega_0))$ such that

$$\begin{aligned} &K(\theta, z; \overline{\eta}, \overline{y}) - \omega^2 M(\theta, z; \overline{\eta}, \overline{y}) \\ &\qquad = \int_{\Omega_0} \left(f(x) \cdot \overline{y}(x) - i\omega\rho_0[\varphi](\phi(x))\, \overline{y}(x) \cdot n(\phi(x)) \right) \sqrt{a(x)}\, dx \end{aligned} \tag{27a}$$

for all $(\eta, y) \in \mathcal{S}$, and

$$\partial_n \varphi(\widetilde{x}) = -i\omega z(x) \cdot n(\widetilde{x}), \qquad \widetilde{x} \in \phi(\Omega_0), \tag{27b}$$

$$\triangle \varphi(\widetilde{x}) + \kappa^2 \varphi(\widetilde{x}) = 0, \qquad \widetilde{x} \in \mathbb{R}^3 \setminus \phi(\Omega_0), \tag{27c}$$

$$\left| \nabla \varphi(\widetilde{x}) \cdot \widetilde{x}/|\widetilde{x}| - i\kappa\varphi(\widetilde{x}) \right| = O\left(1/|\widetilde{x}|^2\right) \qquad \text{as } |\widetilde{x}| \to \infty. \tag{27d}$$

In (27a), the shell is driven by the given function f, specifying a time-harmonic driving force applied to the shell at angular frequency $\omega = c\kappa$, and by the jump $-i\omega\rho_0[\varphi]$ in the air pressure across the shell midsurface (see (20)), where ρ_0 is the density of air.

Existence and uniqueness of solutions to the related problem of 3d elasticity (instead of the Naghdi shell equations) coupled to standard Helmholtz integral equations (instead of the screen integral equation) is addressed in the papers by Bielak, MacCamy, and Zeng [10] and Luke and Martin [43]. Uniqueness can fail in general if the elastic body has a "Jones mode," a free eigenmode that exhibits no surface motion in the normal direction, and thus does not drive the acoustics. This is known to be possible for spheres and axisymmetric structures [43], but almost never happens for general shapes, as shown by Hargé [32], since any sufficiently smooth boundary can be approximated arbitrarily well by shapes that have no Jones modes. Existence and uniqueness results were later proven for other fluid-structure interaction problems. For example, Jentsch, Natroshvili [36, 37] consider an anisotropic inviscid fluid and an anisotropic thermoelastic body. However, it appears that existence and uniqueness of solutions to (27) has not been addressed in the literature. In the following we extend the existence and uniqueness results in [10, 43] to the problem (27).

Jones modes in the context of Nadghi shells are defined as follows.

DEFINITION 2.7. *The pair $(\theta, z) \in \mathcal{S}$, $(\theta, z) \neq 0$ is called a* Jones mode *at frequency ω if*

$$\begin{aligned} K(\theta, z; \overline{\eta}, \overline{y}) - \omega^2 M(\theta, z; \overline{\eta}, \overline{y}) &= 0 \qquad && \text{for all } (\eta, y) \in \mathcal{S}, \\ z(x) \cdot n(\phi(x)) &= 0, && x \in \Omega_0. \end{aligned}$$

The following lemma characterizes conditions required for uniqueness to solutions of (27).

LEMMA 2.8. *Provided that there do not exist any Jones modes at frequency* ω, (27) *has at most one solution.*

Proof. See the Supplement [1]. ∎

With this uniqueness result, the Helmholtz screen problem in (27) can be replaced with the equivalent boundary integral equations (24), where g is given by (18).

The coupled shell structure acoustic problem is given as follows: Find $(\theta, z) \in \mathcal{S}$ and $\psi \in \widetilde{H}^{1/2}(\Omega_0)$ such that

$$K(\theta, z; \overline{\eta}, \overline{y}) - \omega^2 M(\theta, z; \overline{\eta}, \overline{y}) = \int_{\Omega_0} (f \cdot \overline{y} - i\omega\rho_0 \psi \overline{y} \cdot n)\sqrt{a}\, dx, \tag{28a}$$

$$\langle D(\phi)\psi, \overline{\varrho}\rangle_{H^{-1/2}(\Omega_0)\times\widetilde{H}^{1/2}(\Omega_0)} = \int_{\Omega_0} i\omega z \cdot a_3\, \overline{\varrho}\sqrt{a}\, dx \tag{28b}$$

for all $(\eta, y) \in \mathcal{S}$ and all $\varrho \in \widetilde{H}^{1/2}(\Omega_0)$. See (25) for the definition of the differential operator $D(\phi)$ in (28b).

THEOREM 2.9. *Let assumptions* (A1)–(A4) *from section* 2.1 *hold and let* $f \in L^2(\Omega_0)^3$. *If there exist no Jones modes, then there exist a unique solution* $(\theta, z) \in \mathcal{S}$ *and* $\psi \in \widetilde{H}^{1/2}(\Omega_0)$ *solving* (28). *In addition, the solution depends continuously on data, i.e., there exists a constant* $c(\phi) > 0$ *such that*

$$\|(\theta, z)\|_{\mathcal{S}}^2 + \|\phi\|_{\widetilde{H}^{1/2}(\Omega_0))}^2 \le c(\phi)\|f\|_{L^2(\Omega_0)^2}^2 \quad \text{for all } f \in L^2(\Omega_0)^3.$$

Proof. See the Supplement [1]. ∎

For 3d elasticity coupled to the Helmholtz equation (or equivalently, to boundary integral equations), there exist geometries for which Jones modes preclude uniqueness. For shells, this can also happen. For example, if the shell is flat, then the in-plane motions decouple from the out-of-plane motions. The in-plane problem is elliptic, so there will be an infinite sequence of positive increasing eigenvalues, corresponding to purely in-plane motions, which do not drive the acoustics through (28b). If the forcing excites one of these motions, then uniqueness will fail for the coupled problem (28). This situation seems exceedingly unlikely for general curved shells, or for joined shells, where the in-plane motions of one would drive out-of-plane motions of the other.

3. Shell and integral operator differentiability. The bilinear forms (9), (11) in the Naghdi shell equation and the hypersingular operator (25) depend on the thickness t and on the chart ϕ. Ultimately, these two quantities will be design variables, and in section 4 we will determine them to optimize the performance of the coupled shell acoustic system. For this purpose, we establish the Fréchet differentiability of the bilinear forms (9), (11) and of the hypersingular operator (25) with respect to the thickness t and the chart ϕ. The differentiability results will be stated and proven in section 3.1 and section 3.2. We will need the following basic result for the chart functions. In the following lemma, $|\cdot|$ is used to denote both the vector and matrix 2-norm.

LEMMA 3.1. *Let* $\phi \in \mathcal{C}$ *be one-to-one on* $\overline{\Omega}_0$. *If there exists* $\sigma > 0$ *such that*

$$\left|\left(\nabla\phi(x)^T\nabla\phi(x)\right)^{-1}\right| \le \sigma \qquad \forall x \in \Omega_0, \quad \text{then}$$

1. *The function* ϕ *has a Lipschitz-continuous inverse, i.e., there exists a* $c_2 > 0$ *such that* $|x - x'| \le c_2|\phi(x) - \phi(x')|$ *for all* $x, x' \in \Omega_0$.

2. *There exists a constant* $c_1 = c_1(\sigma) > 0$ *such that for any* $h \in W^2_\infty(\Omega_0)^3$ *with* $\|h\|_{W^2_\infty(\Omega_0)^3} < c_1$, *the sum* $\phi + h \in \mathcal{C}$.

Proof. See the Supplement [1]. ∎

3.1. Differentiability of the Naghdi forms. Recall that we use the kinematic assumption (8) on $(\theta, z) \in \mathcal{S}$, defined in (12). This differs from the formulation of the Naghdi model given by Blouza and Le Dret [14] in that it assumes covariant rather than Cartesian components of the rotation angle θ. This allows the space $\mathcal{S}$ to be independent of the chart function ϕ. The overall shape of the shell is given by $g = \mathcal{G} := (\phi, t) \in \mathcal{C} \times \mathcal{T}$; see (4). The shape derivative is written D_g, with component derivatives D_ϕ, D_t. The derivatives are stated in the following theorem.

THEOREM 3.2 (Naghdi shape derivatives). *Let* (A1)–(A4) *hold. If* $\phi \in \mathcal{C}$ *satisfies the assumptions of Lemma* 3.1 *and* $t \in \mathcal{T}$, *then* M, K *are continuously Fréchet differentiable at* $g = (\phi, t)$. *Their Fréchet derivatives* $D_g M(g), D_g K(g) \in \mathcal{L}\left(W^2_\infty(\Omega_0)^3 \times L^\infty(\Omega_0), \mathbb{C}\right)$ *in a direction* $\delta g = (\delta\phi, \delta t) \in W^2_\infty(\Omega_0)^3 \times L^\infty(\Omega_0)$ *are*

$$
\begin{aligned}
D_g M(\theta, z; \eta, y)\delta g = &\int_{\Omega_0} \rho\Big(tz \cdot y + \frac{t^3}{12}\theta_\alpha a^{\alpha\beta}\eta_\beta\Big) D_\phi\sqrt{a}\delta\phi \, dx \\
&+ \int_{\Omega_0} \rho\Big(\delta t z \cdot y + \delta t \frac{t^2}{4}\theta_\alpha a^{\alpha\beta}\eta_\beta\Big)\sqrt{a}\, dx \\
&+ \int_{\Omega_0} \rho\frac{t^3}{12}(\theta_\alpha\eta_\beta D_\phi a^{\alpha\beta})\delta\phi\sqrt{a}\, dx, \\
D_g K(\theta, z; \eta, y)\delta g = &\int_{\Omega_0} \Big(C^{\alpha\beta\lambda\mu}\Big[t\gamma_{\alpha\beta}(z)\gamma_{\lambda\mu}(y) + \frac{t^3}{12}\chi_{\alpha\beta}(\theta, z)\chi_{\lambda\mu}(\eta, y)\Big] \\
&\qquad + tD^{\lambda\mu}\zeta_\lambda(\theta, z)\zeta_\mu(\eta, y)\Big) D_\phi\sqrt{a}\delta\phi \, dx \\
&+ \int_{\Omega_0} \Big(C^{\alpha\beta\lambda\mu}\Big[\delta t\gamma_{\alpha\beta}(z)\gamma_{\lambda\mu}(y) + \frac{t^2\delta t}{4}\chi_{\alpha\beta}(\theta, z)\chi_{\lambda\mu}(\eta, y)\Big] \\
&\qquad + \delta t D^{\lambda\mu}\zeta_\lambda(\theta, z)\zeta_\mu(\eta, y)\Big)\sqrt{a}\, dx \\
&+ \int_{\Omega_0} \Big(D_\phi C^{\alpha\beta\lambda\mu}\Big[t\gamma_{\alpha\beta}(z)\gamma_{\lambda\mu}(z) + \frac{t^3}{12}\chi_{\alpha\beta}(\theta, z)\chi_{\lambda\mu}(\eta, y)\Big] \\
&\qquad + tD_\phi D^{\lambda\mu}\zeta_\lambda(\theta, z)\zeta_\mu(\eta, y)\Big)\delta\phi\sqrt{a}\, dx \\
&+ \int_{\Omega_0} \Big(C^{\alpha\beta\lambda\mu}\Big[tD_\phi(\gamma_{\alpha\beta}(u)\gamma_{\lambda\mu}(v)) + \frac{t^3}{12}D_\phi(\chi_{\alpha\beta}(\theta, z)\chi_{\lambda\mu}(\eta, y))\Big] \\
&\qquad + tD^{\lambda\mu}D_\phi(\zeta_\lambda(\theta, z)\zeta_\mu(\eta, y))\Big)\delta\phi\sqrt{a}\, dx.
\end{aligned}
$$

Proof. If (A1)–(A4) hold and $\phi \in \mathcal{C}$ satisfies the assumptions of Lemma 3.1, then the second part of Lemma 3.1 implies that there exists a $\delta\phi \in W^2_\infty(\Omega_0)$ with $\|\delta\phi\|_{W^2_\infty(\Omega_0)}$ small enough such that $\phi + \delta\phi \in \mathcal{C}$. Let $\delta t \in L^\infty(\Omega_0)$ denote an arbitrary direction with $\|\delta t\|_{L^\infty(\Omega_0)}$ small enough such that $t + \delta t \in \mathcal{T}$. We denote this chart and thickness function pair by $g = (\phi, t)$.

The bilinear forms K (9) and M (11) involve integrals of the form $\int_{\Omega_0} f(x)h[g](x)\, dx$, with $f \in L^1(\Omega_0)$, and $h \in L^\infty(\Omega_0)$ (recall that a are functions of ϕ). Therefore, we consider an integral operator

$$I[g] = \int_{\Omega_0} f(x)h[g](x)\,dx,$$

where $f \in L^1(\Omega_0)$, and $h \in L^\infty(\Omega_0)$ is continuously Fréchet differentiable at g, i.e., there exists a continuous mapping $Dh[g] \in \mathcal{L}\left(W^2_\infty(\Omega_0)^3, L^\infty(\Omega_0)\right)$ such that

$$\|h[g+\delta g] - h[g] - Dh[g]\delta g\|_{L^\infty(\Omega_0)} = o(\|\delta g\|_{W^2_\infty(\Omega_0)^3 \times L^\infty(\Omega_0)}).$$

The derivative is $DI[g]\delta g = \int_{\Omega_0} f(x)Dh[g]\delta g(x)\,dx$, and, indeed,

$$\begin{aligned}|I[g+\delta g] - I[g] - DI[g]\delta g| &= \left|\int_{\Omega_0} f(x)\big(h[g+\delta g](x) - h[g](x) - Dh[g]\delta g(x)\big)\,dx\right| \\ &\le \|f\|_{L^1(\Omega_0)}\|h[g+\delta g] - h[g] - Dh[g]\delta g\|_{L^\infty(\Omega_0)} \\ &= o(\|\delta g\|_{W^2_\infty(\Omega_0)^3 \times L^\infty(\Omega_0)}).\end{aligned}$$

Thus, it is necessary to show continuous Fréchet differentiability of the geometric factors defined in section 2.1, namely of the mappings $\phi \to \sqrt{a}$, $\phi \to a^\alpha$, $\phi \to a^{\alpha\beta}$, and $\phi \to a_i$, $\phi \to \partial_\alpha a_3$. As $t \to t$, $t \to t^3$ are continuously Fréchet differentiable with respect to t, the integrand is continuously Fréchet differentiable with respect to $g = (\phi, t)$.

The map $a_\alpha \in W^1_\infty(\Omega_0)^3$ of the chart to the covariant basis vectors has Fréchet derivative at ϕ

$$D_\phi a_\alpha \delta\phi = \partial_\alpha \delta\phi.$$

The covariant components $a_{\alpha\beta} := a_\alpha \cdot a_\beta \in W^1_\infty(\Omega_0)$ of the metric tensor have Fréchet derivative

$$D_\phi a_{\alpha\beta} = a_\beta \cdot D_\phi a_\alpha + a_\alpha \cdot D_\phi a_\beta,$$

which can be used to express the derivative of change of metric factor $\sqrt{a} := \sqrt{a_{11}a_{22} - a_{12}^2} \in W^1_\infty(\Omega_0)$ via

$$D_\phi\sqrt{a} = (2\sqrt{a})^{-1}(a_{22}D_\phi a_{11} + a_{11}D_\phi a_{22} - 2a_{12}D_\phi a_{12}) =: (2\sqrt{a})^{-1}D_\phi a.$$

The contravariant components

$$(a^{\alpha\beta}) = \begin{pmatrix} a^{11} & a^{12} \\ a^{21} & a^{22}\end{pmatrix} := (a_{\alpha\beta})^{-1} = \frac{1}{\sqrt{a}^2}\begin{pmatrix} a_{22} & -a_{12} \\ -a_{21} & a_{11}\end{pmatrix} \in W^1_\infty(\Omega)$$

have Fréchet derivatives

$$\begin{pmatrix} D_\phi a^{11} \\ D_\phi a^{12} \\ D_\phi a^{22}\end{pmatrix} = \frac{1}{\sqrt{a}^2}\begin{pmatrix} D_\phi a_{22} \\ -D_\phi a_{12} \\ D_\phi a_{11}\end{pmatrix} + \frac{1}{\sqrt{a}^4}\begin{pmatrix} -a_{22} \\ a_{12} \\ -a_{11}\end{pmatrix} D_\phi a.$$

It remains to address the normal vector $a_3 \in W^1_\infty(\Omega_0)^3$, the dual basis vectors $a^\alpha \in W^1_\infty(\Omega_0)^3$, and the term $\partial_\alpha a_3 \in L^\infty(\Omega_0)$ (related to surface curvature). Unlike those terms discussed thus far, these are not directly used in the finite element implementation of general shell models; see [16, section 6.3]). Because it is

needed later for Theorem 3.4, we state the Fréchet derivative of the normal vector $a_3 := (a_1 \times a_2)/|a_1 \times a_2|$:

$$D_\phi a_3 = \frac{D_\phi a_1 \times a_2 + a_1 \times D_\phi a_2}{|a_1 \times a_2|} - \frac{a_1 \times a_2}{|a_1 \times a_2|^2} \frac{(a_1 \times a_2)^T}{|a_1 \times a_2|} (D_\phi a_1 \times a_2 + a_1 \times D_\phi a_2)$$
$$= |a_1 \times a_2|^{-1} \left(I - a_3 a_3^T \right) (D_\phi a_1 \times a_2 + a_1 \times D_\phi a_2). \qquad \square$$

PROPOSITION 3.3. *The forcing terms (assuming that the loading f is independent of ϕ) require only differentiation of $\sqrt{a}$ and a_3:*

$$D_g \Big(\int_{\Omega_0} \left(f \cdot \overline{y} - i\omega \rho_0 [\varphi] \overline{y} \cdot a_3 \right) \sqrt{a}\, dx \Big) \delta g = \int_{\Omega_0} \left(f \cdot \overline{y} - i\omega \rho_0 [\varphi] \overline{y} \cdot a_3 \right) D_\phi \sqrt{a} \delta\phi\, dx$$
$$- \int_{\Omega_0} i\omega \rho_0 [\varphi] \overline{y} \cdot D_\phi a_3 \sqrt{a} \delta\phi\, dx,$$
$$D_g \Big(\int_{\Omega_0} i\omega \overline{\varrho} z \cdot a_3 \sqrt{a}\, dx \Big) \delta g = \int_{\Omega_0} i\omega \overline{\varrho} z \cdot \left(a_3 D_\phi \sqrt{a} + \sqrt{a} D_\phi a_3 \right) \delta\phi\, dx.$$

3.2. Shape differentiation of the hypersingular operator. While one might expect that shape differentiation would increase the order of the kernel singularity of the integral, it turns out that, for W^2_∞ surfaces, the singularity remains of the same order. We refer to Potthast [51, 52] for a similar result for C^2 surfaces. This is crucial for the Fréchet differentiability for the weak form of the hypersingular operator, which will be established next. In the following theorem, recall that

$$G(\phi(x), \phi(x')) = \frac{\exp(i\kappa |\phi(x) - \phi(x')|)}{4\pi |\phi(x) - \phi(x')|} = \frac{\exp(i\kappa r(x, x'))}{4\pi r(x, x')}$$

with $r(x, x') = |\phi(x) - \phi(x')|$.

THEOREM 3.4 (Hypersingular operator shape derivatives). *Let* (A1)–(A4) *hold. If $\phi \in \mathcal{C}$ satisfies the assumptions of Lemma* 3.1*, then the map $\langle D(\cdot)\psi, \varrho \rangle_{\Omega_0}$ in* (25) *is continuously Fréchet differentiable at ϕ and the Fréchet derivative at ϕ is an operator $D_\phi \langle D(\phi)\psi, \varrho \rangle_{\Omega_0} \in \mathcal{L}\left(W^2_\infty(\Omega_0)^3, \mathbb{C} \right)$. Using the abbreviations $G(\bullet) = G(\phi(x), \phi(x'))$,*

$$\frac{\partial G}{\partial r}(\bullet) = \frac{\partial}{\partial r} \left(\frac{\exp(i\kappa r)}{4\pi r} \right) \Big|_{r = |\phi(x) - \phi(x')|}$$

and

$$\frac{\partial r}{\partial \phi}(\bullet)\delta\phi = \frac{\phi(x) - \phi(x')}{|\phi(x) - \phi(x')|} \cdot \left(\delta\phi(x) - \delta\phi(x') \right),$$

and recalling that $a_3(x), a_3(x')$, $\sqrt{a(x)}, \sqrt{a(x')}$ given by (3) *depend on ϕ, the derivative in a direction $\delta\phi \in W^2_\infty(\Omega_0)^3$ is given by*

$$D_\phi \langle D(\phi)\psi, \varrho \rangle_{\Omega_0} \delta\phi = \iint_{\Omega_0} \Big(\frac{\partial G}{\partial r}(\bullet) \frac{\partial r}{\partial \phi}(\bullet) \delta\phi (a_3(x') \times \nabla\Phi^{-T}(x) \widetilde{\nabla} \psi(x'))$$
$$\times (a_3(x) \times \nabla\Phi^{-T}(x) \widetilde{\nabla} \varrho(x))$$
$$+ G(\bullet) D_\phi ((a_3(x') \times \nabla\Phi^{-T}(x) \widetilde{\nabla} \psi(x'))$$
$$\times (a_3(x) \times \nabla\Phi^{-T}(x) \widetilde{\nabla} \varrho(x))) \delta\phi \Big)$$
$$\times \sqrt{a(x')a(x)}\, dx' dx$$

$$
\begin{aligned}
&- \kappa^2 \iint_{\Omega_0} \Big(\frac{\partial G}{\partial r}(\bullet) \frac{\partial r}{\partial \phi}(\bullet)(a_3(x')\psi(x')) \cdot (a_3(x)\varrho(x)) \\
&\qquad + G(\bullet)\psi(x')\varrho(x) D_\phi(a_3(x') \cdot a_3(x)) \Big) \\
&\qquad \times \delta\phi \sqrt{a(x')a(x)}\, dx' dx \\
&+ \iint_{\Omega_0} G(\bullet)(a_3(x') \times \nabla\Phi^{-T}(x)\widetilde{\nabla}\psi(x')) \\
&\qquad \times (a_3(x) \times \nabla\Phi^{-T}(x)\widetilde{\nabla}\varrho(x)) \\
&\qquad \times D_\phi(\sqrt{a(x')a(x)})\delta\phi\, dx' dx \\
&- \kappa^2 \iint_{\Omega_0} G(\bullet)(a_3(x')\psi(x')) \\
&\qquad \times (a_3(x)\varrho(x)) D_\phi(\sqrt{a(x')a(x)})\delta\phi\, dx' dx. \qquad (29)
\end{aligned}
$$

Proof. Let $\phi \in \mathcal{C}$ satisfy the assumptions of Lemma 3.1, and let $\delta\phi \in W^2_\infty(\Omega_0)^3$ denote an arbitrary direction with $\|\delta\phi\|_{W^2_\infty(\Omega_0)}$ small enough such that for $\phi + \delta\phi \in \mathcal{C}$. For a fixed $(x, x') \in \Omega_0 \times \Omega_0$ with $x \neq x'$, we have $\phi(x) \neq \phi(x')$. Thus the mapping

$$G : \mathcal{C} \to \mathbb{C}, \qquad \phi \mapsto G(\bullet) := G(\phi(x), \phi(x'))$$

is continuously Fréchet differentiable. Indeed, $\widetilde{g}_{x,x'} : \mathcal{C} \to \mathbb{R}^3$ defined by

$$\widetilde{g}_{x,x'} := \phi(x) - \phi(x')$$

is a linear mapping. It is continuously Fréchet differentiable with derivative

$$D_\phi \widetilde{g}_{x,x'}(\phi)\delta\phi = \delta\phi(x) - \delta\phi(x'), \quad \delta\phi \in W^2_\infty(\Omega).$$

Since $\phi(x) \neq \phi(x')$, using the chain rule we obtain the Fréchet differentiability of the mapping $\widehat{g}_{x,x'} : \mathcal{C} \to \mathbb{R}, \quad \phi \mapsto |\phi(x) - \phi(x')|$, and the Fréchet derivative is given by

$$D_\phi \widehat{g}_{x,x'}(\phi)\delta\phi = |\phi(x) - \phi(x')|^{-1}(\phi(x) - \phi(x')) \cdot (\delta\phi(x) - \delta\phi(x')).$$

It then follows that the Fréchet derivative of G in direction $\delta\phi$ is given by

$$
\begin{aligned}
D_\phi G(\phi(x), \phi(x'))\delta\phi = \frac{1}{4\pi} \Big(\frac{i\kappa \left(\phi(x) - \phi(x')\right)}{\left|\phi(x) - \phi(x')\right|} - \frac{\phi(x) - \phi(x')}{\left|\phi(x) - \phi(x')\right|^3} \Big) \\
\cdot \exp\left(i\kappa \left|\phi(x) - \phi(x')\right|\right) \left(\delta\phi(x) - \delta\phi(x')\right).
\end{aligned}
$$

Potthast in [51, Lemma. 1] shows that order of singularity for $D_\phi G$ is same as G in the Hölder space setting. A similar assertion holds in our case as well.

Using Lemma 3.1, there exists a constant $c_1(\phi) > 0$ such that for every $x, x' \in \Omega_0$

$$\left|x - x'\right| \leq c_1(\phi) \left|\phi(x) - \phi(x')\right|.$$

Since $\delta\phi$ is in $W^2_\infty(\Omega_0)^3$, it is Lipschitz continuous, $\left|\delta\phi(x) - \delta\phi(x')\right| \leq c_2 \left|x - x'\right|$. Hence

$$
\begin{aligned}
\left|D_\phi G(\phi(x), \phi(x'))\delta\phi\right| &\leq C\Big(1 + \left|\phi(x) - \phi(x')\right|^{-2}\Big) \left|\delta\phi(x) - \delta\phi(x')\right| \\
&\leq C\Big(1 + \left|x - x'\right|^{-2}\Big) \left|x - x'\right|,
\end{aligned}
$$

where $C > 0$ denotes a generic constant which depends on ϕ. We have shown that the kernel remains weakly singular after Fréchet differentiation. The integrand in (29) therefore includes integrable kernels multiplied against a function composed of geometric factors, the vector operations $\cdot$ and $\times$, and the functions ψ, ϱ. It is established in the proof of Theorem 3.2 that the geometric terms $\sqrt{a}$, a_i are continuously Fréchet differentiable with respect to ϕ, and thus, by the same argument, the derivative must be as stated above. ∎

4. Transfer function optimization. Recall that the shape of the Naghdi shell is determined by the middle-surface chart function $\phi \in \mathcal{C}$, and the thickness function $t \in \mathcal{T}$. These parameters are denoted by

$$g = (\phi, t) \in \mathcal{G} := \mathcal{C} \times \mathcal{T}.$$

Given a shape parameter $g \in \mathcal{G}$, we consider the coupled shell acoustic equation (28). Recall the definitions (12) of $\mathcal{S}$ and (22) of $\widetilde{H}^{1/2}(\Omega_0)$. The solution (if it exists)

$$U = (\psi, \theta, z)$$

of the coupled shell acoustic equation (28) is in the state space

$$\mathcal{U} = \widetilde{H}^{1/2}(\Omega_0) \times \mathcal{S}.$$

Given $\omega > 0$, we define a constraint function $c : \mathcal{G} \times \mathcal{U} \to \mathcal{U}'$ by

$$\begin{aligned} \langle c(g, U; \omega), V \rangle_{\mathcal{U}' \times \mathcal{U}} = {} & K(\theta, z; \overline{\eta}, \overline{y}) - \omega^2 M(\theta, z; \overline{\eta}, \overline{y}) \\ & - \int_{\Omega_0} (f \cdot \overline{y} - i\omega\rho_0 \psi \overline{y} \cdot n) \sqrt{a}\, dx \\ & + \langle D(\phi)\psi, \overline{\varrho} \rangle_{H^{-1/2}(\Omega_0) \times \widetilde{H}^{1/2}(\Omega_0)} \\ & - \int_{\Omega_0} i\omega z(x) \cdot a_3(x)\, \overline{\varrho}(x) \sqrt{a}\, dx, \end{aligned} \tag{30}$$

where $U = (\psi, \theta, z)$ and $V = (\varrho, \eta, y)$. The coupled shell acoustic equation (28) is equivalent to solving

$$c(g, U; \omega) = 0 \in \mathcal{U}'.$$

The specific objective function we consider measures the deviation of the response at the external point $x^* \in \mathbb{R}^3 \setminus \phi(\Omega_0)$ from the desired acoustic response over N_ω discrete frequencies. For a given frequency $\omega > 0$, the response at the external point $x^* \in \mathbb{R}^3 \setminus \phi(\Omega_0)$ is given by the representation formula (cf. (21))

$$R(g, U; \omega) = \int_{\Omega_0} \frac{\partial G(\phi(x), x^*)}{\partial a_3} \psi \sqrt{a}\, dx, \tag{31}$$

where $g = (\phi, t)$ and $U = (\psi, \theta, z)$.

Defining

$$j_k(g, U; \omega_k) = \tfrac{1}{2}(|R(g, U; \omega_k)| - r_k)^2 \tag{32}$$

as the composition of R with the continuous function $\frac{1}{2}(|\cdot| - r_k)^2 : \mathbb{C} \to \mathbb{R}$ (here $|\cdot| : \mathbb{C} \to \mathbb{R}^+$ denotes the complex modulus function), our objective is the weighted sum of squares

$$j(g, U[g;\omega_1], \ldots, U[g;\omega_{N_\omega}]) = \sum_{k=1}^{N_\omega} \alpha_k j_k(g, U[g;\omega_k];\omega_k), \tag{33}$$

where $r_1, \ldots, r_{N_\omega} \in \mathbb{R}^+$ are the desired acoustic responses, $\alpha_1, \ldots, \alpha_{N_\omega} \in \mathbb{R}^+$ are positive weights, and g and $U[g;\omega_k]$ will be related through the coupled shell acoustic equation (30) at frequency ω_k.

Given a set $\mathcal{G}_{ad} \subset \mathcal{G}$ of admissible shapes, we want to solve

$$\text{minimize } j(g, U[\omega_1], \ldots, U[\omega_{N_\omega}]), \tag{34a}$$

$$\text{subject to } c(g, U[\omega_k];\omega_k) = 0 \in \mathcal{U}', \quad k = 1, \ldots, N_\omega, \tag{34b}$$

$$g \in \mathcal{G}_{ad}. \tag{34c}$$

To ensure well-posedness of (34), we need to specify the set $\mathcal{G}_{ad}$ of admissible shapes. It turns out that we also need to add a constraint. We will analyze existence of solutions in section 4.1, and gradient computation using the adjoint equations in section 4.2.

4.1. Existence of optimal solutions. First we specify the set $\mathcal{G}_{ad}$ of admissible shapes. In their paper [34] on plate thickness optimization Hlavacek and Lovisek use as the set $\mathcal{T}_{ad}$ of admissible thickness functions the set of Lipschitz-continuous functions whose Lipschitz constants are bounded by a given constant $L > 0$. This set is compact. In [2], Sprekels et al. prove the existence of solutions to a class (the chart ϕ is assumed to be a graph) of mechanical shell shape optimization problems for $\phi \in C^2(\overline{\Omega}_0)$. They assume the constraint set to be compact [2, Cor. 6.5] with respect to the C^2 topology, without stating conditions under which this will be true.

Recall the set $\mathcal{T}$ defined in (14). For given $l_1 > 0$ and $p \in (2, \infty)$ we define the set of admissible thicknesses

$$\mathcal{T}_{ad} := \mathcal{T} \cap \left\{ t \in W_p^1(\Omega_0) : \|t\|_{W_p^1(\Omega_0)} \le l_1 \right\}. \tag{35a}$$

The set of admissible thicknesses $\mathcal{T}_{ad}$ is closed, convex, and bounded, and therefore weakly sequentially compact with respect to the W_p^1 topology. Moreover, by the Sobolev embedding theorem the set $\mathcal{T}_{ad}$ is compact with respect to the L^∞ topology. Since for $p > 2$, $W_p^1(\Omega_0) \subset C^{0,1-2/p}(\overline{\Omega}_0)$, our condition on the thicknesses is slightly weaker than that in [34].

The construction of $\mathcal{C}_{ad}$ is a bit more involved. Let $\widehat{\mathcal{C}}$ be a closed and convex subset of the set $\mathcal{C}$ of charts defined in (2). One example for $\widehat{\mathcal{C}}$ is the set of charts $\phi = (x_1, x_2, \zeta(x_1, x_2))$, where ζ is a sufficiently smooth function. The charts in this set are graphs with ζ denoting the height. This example (with smoothness assumptions on ϕ, i.e., ζ, different from those we will impose below) is used in [2, eq. 5.1]. Another example is the set $\widehat{\mathcal{C}} = \{\phi \in W_\infty^2(\Omega_0)^3 : \|\phi - \phi_0\|_{W_\infty^2(\Omega_0)^3} \le c\}$, where $\phi_0 \in \mathcal{C}$ is a chart that satisfies the assumptions of Lemma 3.1 and $c > 0$ is sufficiently small to ensure $\widehat{\mathcal{C}} \subset \mathcal{C}$; see Lemma 3.1. For given $l_2 > 0$ and the same $p \in (2, \infty)$ used before, we define the set of admissible charts

$$\mathcal{C}_{ad} := \widehat{\mathcal{C}} \cap \left\{ \phi \in W_p^3(\Omega_0)^3 : \|\phi\|_{W_p^3(\Omega_0)^3} \le l_2 \right\}. \tag{35b}$$

The set $\mathcal{C}_{ad}$ is a closed, convex, and bounded subset of the reflexive Banach space $W_p^3(\Omega_0)^3$ and is therefore weakly sequentially compact with respect to the W_p^3 topology and, by the Sobolev embedding theorem, compact with respect to the W_∞^2 topology. Since $W_p^3(\Omega_0) \subset C^{2,1-2/p}(\overline{\Omega}_0)$, our chart functions are slightly more regular than

the C^2 charts used in [2], but our set of admissible charts is constructed to have the appropriate compactness properties.

The set of admissible shapes is

$$\mathcal{G}_{ad} = \mathcal{C}_{ad} \times \mathcal{T}_{ad}. \tag{35c}$$

The objective function (33) involves a solution $U[g;\omega]$ of $c(g,U;\omega)=0$. But for a general (g,ω), there may be Jones modes, and the solution may not be unique, or for that matter may not even exist. Therefore, existence of minimizers of the objective function (33) cannot immediately be established for the set $\mathcal{G}_{ad}$ of admissible shapes. One might hope that the objective function would help to avoid any difficulties with nonexistence or nonuniqueness of the state equation. However, any objective function that depends only on the acoustic field produced by the vibrating shell structure (such as in (33)) is insensitive to Jones modes, because they do not radiate sound. If there exists a shape g_* that produces exactly the response data the objective function seeks to match, and the shape g_* has a Jones mode that is driven by the forcing, $g_k \to g_*$, and $c(g_k,U_k;\omega)=0$, then $\|U_k\|_{\mathcal{U}}$ will be unbounded. We will illustrate this in the Supplement [1] with a simple 1d example.

The potential difficulties arising from Jones modes can be overcome by adding constraints

$$\|U[g;\omega_k]\|_{\mathcal{U}} \le M, \quad k=1,\dots,N_\omega. \tag{36}$$

These constraints (36) serve as a means of detecting Jones modes that affect the results of the optimization. The bound M is chosen to be so large that the constraint only becomes active when the shape approaches a shape with a Jones mode excited by the forcing, in which case it is necessary to modify the forcing or the objective function: in practice, we are not interested in optimal solutions where (36) is active.

Instead of (34) the optimization problem is now

$$\text{minimize } j(g,U[\omega_1],\dots,U[\omega_{N_\omega}]), \tag{37a}$$

$$\text{subject to } c(g,U[\omega_k];\omega_k)=0\in\mathcal{U}', \quad k=1,\dots,N_\omega, \tag{37b}$$

$$\|U[\omega_k]\|_{\mathcal{U}} \le M, \quad k=1,\dots,N_\omega, \tag{37c}$$

$$g\in\mathcal{G}_{ad}. \tag{37d}$$

THEOREM 4.1. *Let assumptions* (A1)–(A4) *hold and let* $\mathcal{G}_{ad}$ *be given by* (35). *If* $j(g,U[\omega_1],\dots,U[\omega_{N_\omega}])$ *is bounded below on the set of feasible points*

$$\mathcal{F}=\{(g,U[\omega_1],\dots,U[\omega_{N_\omega}])\in\mathcal{G}_{ad}\times\mathcal{U} \,:\, U[\omega_1],\dots,\|U[\omega_{N_\omega}] \text{ satisfy } (37b),(37c)\}$$

and weakly lower semicontinuous in the sense that if $g_n \to g$ *in* $W^2_\infty(\Omega_0)^3 \times L^\infty(\Omega_0)$ *and* $U_n[\omega_k] \rightharpoonup U[\omega_k]$ *in* $\mathcal{U}$, $k=1,\dots,N_\omega$, *then* $j(g,U[\omega_1],\dots,U[\omega_{N_\omega}]) \le \liminf_{n\to\infty} j(g_n,U_n[\omega_1],\dots,U_n[\omega_{N_\omega}])$, *then the problem* (37) *has a solution.*

Proof. To simplify the notation, it is sufficient to consider case of one frequency $N_\omega=1$ and to drop $[\omega_1]$ from the notation of U.

Under the assumption that j is bounded below, there exists a sequence $(g_n,U_n)_{n\in\mathbb{N}}$ of feasible points such that

$$j(g_n,U_n) \to \inf_{(g,U)\in\mathcal{F}} j(g,U).$$

Assumptions (A2), (A4) imply that $\mathcal{G}_{ad}$ is a closed, convex, bounded, and nonempty subset of $W_p^3(\Omega_0)^3 \times W_p^1(\Omega_0)$. Moreover, $\mathcal{G}_{ad}$ is weakly sequentially compact in $W_p^3(\Omega_0)^3 \times W_p^1(\Omega_0)$ and compact in $W_\infty^2(\Omega_0)^3 \times L^\infty(\Omega_0)$. Consequently there exists a subsequence (still denoted by g_n) such that

$$g_n \to g_* \text{ in } W_\infty^2(\Omega_0)^3 \times L^\infty(\Omega_0), \quad \text{with } g_* \in \mathcal{G}_{ad}.$$

We will show that g_* is an optimal shape. To this end, we note that $\{U \in \mathcal{U} : \|U\|_{\mathcal{U}} \leq M\}$ is a closed, convex, bounded subset of $\mathcal{U}$, and therefore there exists a weakly convergent subsequence (still denoted by U_n) such that

$$U_n \rightharpoonup U_* \text{ in } \mathcal{U}, \quad \text{with } \|U_*\|_{\mathcal{U}} \leq M.$$

Using weak lower semicontinuity of the objective j,

$$\inf_{(g,U)\in\mathcal{F}} j(g,U) \leq j(g_*,U_*) \leq \liminf_{n\to\infty} j(g_n,U_n) = \inf_{(g,U)\in\mathcal{F}} j(g,U).$$

It remains only to show that that $c(g_*,U_*;\omega) = 0$, and therefore that (g_*,U_*) is a solution to the optimization problem (37).

For given $V \in \mathcal{U}$, $\langle c(g,U;\omega),V\rangle_{\mathcal{U}'\times\mathcal{U}}$ consists of integrals of the form $\int_{\Omega_0} f(x)\, h[g](x)w(x)\,dx$, where $f \in L^2(\Omega_0)$ depends on U and its derivatives, $h \in L^\infty(\Omega_0)$ is a function of the shape g, and $w \in L^2(\Omega_0)$. Furthermore, if $U_n \rightharpoonup U_* \in \mathcal{U}$, then the corresponding functions f_n, f_* satisfy $f_n \rightharpoonup f_* \in L^2(\Omega_0)$. Moreover, if $g_n \to g_*$ in $W_\infty^2(\Omega_0)^3 \times L^\infty(\Omega_0)$, then $h(g_n) \to h(g_*)$ in $L^\infty(\Omega_0)$. Therefore, to prove $0 = c(g_n,U_n;\omega) \to c(g_*,U_*;\omega)$ (and therefore $c(g_*,U_*;\omega) = 0$), it is sufficient to prove that $f_n \rightharpoonup f_* \in L^2(\Omega_0)$ and $h(g_n) \to h(g_*)$ in $L_\infty(\Omega_0)$ imply $\int_{\Omega_0} f_n(x)h[g_n](x)w(x)\,dx \to \int_{\Omega_0} f_*(x)h[g_*](x)w(x)\,dx$. Applying the triangle inequality gives $\left|\int_{\Omega_0} f_n(x)h[g_n](x)w(x) - f_*(x)h[g_*](x)w(x)\right| \leq \left|\int_{\Omega_0} f_n(x)(h[g_n](x)-h[g_*](x))w(x)\right| + \left|\int_{\Omega_0}(f_n(x)-f_*(x))h[g_*](x)w(x)\right|$. Using the Cauchy–Schwarz inequality and the fact that $\{f_n\}_{n=1}^\infty$ is bounded in L^2 implies that the first term on the right-hand side converges to zero. The convergence of the second term to zero is a direct consequence of the definition of a weak limit. ∎

We now address applicability of Theorem 4.1 to (33). The weak lower semicontinuity of the objective function j, (32), (33), in the sense that if $g_n \to g$ in $W_\infty^2(\Omega_0)^3 \times L^\infty(\Omega_0)$ and $U_n \rightharpoonup U$ in $\mathcal{U}$, then $j(g,U) \leq \liminf_{n\to\infty} j(g_n,U_n)$ follows from the following theorem and the definition (31), (32), (33) of j.

THEOREM 4.2. *Let assumptions* (A1) *and* (A2) *hold. If* $U_n \rightharpoonup U_*$ *in* $\mathcal{U}$ *and* $g_n \to g_*$ *in* $W_\infty^2(\Omega_0)^3 \times L^\infty(\Omega_0)$, *then* $R(g_n,U_n;\omega_k) \to R(g_*,U_*;\omega_k)$.

Proof. This can be established by applying the arguments that were used in the proof of Theorem 4.1 to show that $c(g_n,U_n;\omega) \to c(g_*,U_*;\omega)$. ∎

In practice we often consider the implicitly constrained version of (37). Assume that (37b) have unique solutions $U[g;\omega_k]$, define

$$J(g) = j(g,U[g,\omega_1],\ldots,U[g,\omega_{N_\omega}]), \tag{38}$$

and instead of (37), consider

$$\text{minimize } J(g), \tag{39a}$$

$$\text{subject to } \|U[g,\omega_k]\|_{\mathcal{U}} \leq M, \quad k = 1,\ldots,N_\omega, \tag{39b}$$

$$g \in \mathcal{G}_{ad}. \tag{39c}$$

Next we discuss the computation of the gradient of the objective function in (39).

4.2. Gradient computations. The objective function (33), (38) is a mapping $J : \mathcal{G}_{ad} \to \mathbb{R}$. Each term (32) in the sum is a composition of the following mappings:

$$g \to U \to R \to \tfrac{1}{2}(|\cdot| - r_k)^2$$

(cf. (32)). The composition J is a nonlinear functional on the real-valued Banach space $\mathcal{G}$, but U and R are functions in complex-valued Banach spaces. To differentiate the nonlinear functional J we identify the complex-valued functions with pairs of real valued functions, the real and imaginary parts of the complex-valued functions. In practice, however, it is often beneficial to work with complex-valued functions and this creates subtle issues in the computation of the gradient. We will illustrate this first using a simple example.

EXAMPLE 4.3. *Let* $\mathbf{A}(\mathbf{g}) \in \mathbb{C}^{n\times n}$ *be invertible for every* $\mathbf{g} \in \mathbb{R}^m$*, and let* $\mathbf{b} \in \mathbb{C}^n$*,* $\mathbf{r} \in \mathbb{C}^n$ *be given. Let* $\mathbf{u}(\mathbf{g}) \in \mathbb{C}^n$ *be the solution of*

$$\mathbf{A}(\mathbf{g})\mathbf{u} = \mathbf{b} \tag{40}$$

and consider the function $J : \mathbb{R}^m \to \mathbb{R}$ *defined by*

$$J(\mathbf{g}) = |\mathbf{r}^*\mathbf{u}(\mathbf{g})|. \tag{41}$$

This example mimics the objective function (33) *for a single frequency. In fact, this example problem is very close to a discretized version of our problem. The vector* $\mathbf{g} \in \mathbb{R}^m$ *corresponds to a parametrization of the shell geometry. The linear system* $\mathbf{A}(\mathbf{g})\mathbf{u} = \mathbf{b}$ *plays the role of the coupled shell acoustic system, and* $\mathbf{r}^*\mathbf{u}$ *plays the role of the representation operator. (A discrete version of the representation operator depends on* $\mathbf{g}$*, but this added complexity would distract from the adjoint computation issue we want to illustrate with this example.)*

We use the subscripts R *and* I *to denote the real and imaginary part of a complex matrix, vector, or number and write the complex linear system* $\mathbf{A}(\mathbf{g})\mathbf{u} = \mathbf{b}$ *as*

$$\begin{pmatrix} \mathbf{A}(\mathbf{g})_R & -\mathbf{A}(\mathbf{g})_I \\ \mathbf{A}(\mathbf{g})_I & \mathbf{A}(\mathbf{g})_R \end{pmatrix} \begin{pmatrix} \mathbf{u}_R \\ \mathbf{u}_I \end{pmatrix} = \begin{pmatrix} \mathbf{b}_R \\ \mathbf{b}_I \end{pmatrix}. \tag{42}$$

To simplify notation, we use an underbar to denote the real matrices and vectors and write the previous system as

$$\underline{\mathbf{A}}(\mathbf{g})\underline{\mathbf{u}} = \underline{\mathbf{b}}. \tag{43}$$

Similarly, we can write $\mathbf{r}^*\mathbf{u}$ *as*

$$\begin{pmatrix} \mathbf{r}_R^T\mathbf{u}_R + \mathbf{r}_I^T\mathbf{u}_I \\ \mathbf{r}_R^T\mathbf{u}_I - \mathbf{r}_I^T\mathbf{u}_R \end{pmatrix} = \begin{pmatrix} \mathbf{r}_R^T & \mathbf{r}_I^T \\ \mathbf{r}_R^T & -\mathbf{r}_I^T \end{pmatrix} \begin{pmatrix} \mathbf{u}_R \\ \mathbf{u}_I \end{pmatrix} \stackrel{\text{def}}{=} \underline{\mathbf{R}}\,\underline{\mathbf{u}},$$

where $\underline{\mathbf{R}} \in \mathbb{R}^{2\times 2n}$*. Let* $\underline{\mathbf{u}}(\mathbf{g}) \in \mathbb{R}^{2n}$ *denote the solution of* (43)*. The objective function* (41) *can now be written as*

$$J(\mathbf{g}) = \|\underline{\mathbf{R}}\,\underline{\mathbf{u}}(\mathbf{g})\|_2. \tag{44}$$

If $\mathbb{R}^m \ni \mathbf{g} \to \mathbf{A}_R(\mathbf{g}), \mathbf{A}_I(\mathbf{g}) \in \mathbb{R}^{n\times n}$ *are Fréchet differentiable, and* $\underline{\mathbf{R}}\,\underline{\mathbf{u}}(\mathbf{g}) \neq 0$*, then the function* (44) *is Fréchet differentiable, and its Fréchet derivative at* $\mathbf{g}$ *in the direction* $\delta\mathbf{g}$ *is given by*

$$DJ(\mathbf{g})\,\delta\mathbf{g} = \frac{1}{\|\underline{\mathbf{R}}\,\underline{\mathbf{u}}(\mathbf{g})\|_2}\underline{\mathbf{u}}(\mathbf{g})^T\underline{\mathbf{R}}^T\underline{\mathbf{R}}\,D_{\mathbf{g}}\underline{\mathbf{u}}(\mathbf{g})\;\delta\mathbf{g}$$

$$= -\frac{1}{\|\underline{\mathbf{R}}\,\underline{\mathbf{u}}(\mathbf{g})\|_2}\underline{\mathbf{u}}(\mathbf{g})^T\underline{\mathbf{R}}^T\underline{\mathbf{R}}\,\underline{\mathbf{A}}(\mathbf{g})^{-1}D_{\mathbf{g}}(\underline{\mathbf{A}}(\mathbf{g})\underline{\mathbf{u}})|_{\underline{\mathbf{u}}=\underline{\mathbf{u}}(\mathbf{g})}\;\delta\mathbf{g}. \tag{45}$$

The gradient of J is the vector $\nabla J(\mathbf{g}) \in \mathbb{R}^m$ such that $\nabla J(\mathbf{g})^T\delta\mathbf{g} = DJ(\mathbf{g})\,\delta\mathbf{g}$ for all $\delta\mathbf{g} \in \mathbb{R}^m$. If we define $\mathbf{p} \in \mathbb{R}^{2n}$ as the solution of the adjoint equation

$$\underline{\mathbf{A}}(\mathbf{g})\mathbf{p} = -\frac{1}{\|\underline{\mathbf{R}}\,\underline{\mathbf{u}}(\mathbf{g})\|_2}\underline{\mathbf{R}}^T\underline{\mathbf{R}}\,\underline{\mathbf{u}}(\mathbf{g})$$

then

$$\nabla J(\mathbf{g})^T\delta\mathbf{g} = DJ(\mathbf{g})\,\delta\mathbf{g} = \mathbf{p}^T D_{\mathbf{g}}(\underline{\mathbf{A}}(\mathbf{g})\underline{\mathbf{u}})|_{\underline{\mathbf{u}}=\underline{\mathbf{u}}(\mathbf{g})}\;\delta\mathbf{g}$$

for all $\delta\mathbf{g} \in \mathbb{R}^m$ and, consequently,

$$\nabla J(\mathbf{g}) = \Big(D_{\mathbf{g}}(\underline{\mathbf{A}}(\mathbf{g})\underline{\mathbf{u}})|_{\underline{\mathbf{u}}=\underline{\mathbf{u}}(\mathbf{g})}\Big)^T\mathbf{p}. \tag{46}$$

The previous calculus requires representation of complex numbers as real vectors. For computational purposes it is often favorable to avoid this conversion and we therefore want to derive the gradient using the original representations (40) *and* (41).

The real derivative (see [53, *Chap.* 1, *section* 2]*) of $|\cdot| : \mathbb{C} \to \mathbb{R}$ at a point $z = x + iy \in \mathbb{C}\setminus\{0\}$, in a direction $\delta z = \delta x + i\delta y$ is given by*

$$D|z|\,\delta z = \frac{x\delta x + y\delta y}{\sqrt{x^2+y^2}}. \tag{47}$$

If $|\mathbf{r}^*\mathbf{u}(\mathbf{g})| > 0$, then the function (41) *is Fréchet differentiable, and its Fréchet derivative at $\mathbf{g}$ in the direction $\delta\mathbf{g}$ is given by*

$$DJ(\mathbf{g})\,\delta\mathbf{g} = D|\mathbf{r}^*\mathbf{u}(\mathbf{g})|\;\mathbf{r}^*D_{\mathbf{g}}\mathbf{u}(\mathbf{g})\;\delta\mathbf{g}$$

$$= -D|\mathbf{r}^*\mathbf{u}(\mathbf{g})|\;\mathbf{r}^*\mathbf{A}(\mathbf{g})^{-1}D_{\mathbf{g}}(\mathbf{A}(\mathbf{g})\mathbf{u})|_{\mathbf{u}=\mathbf{u}(\mathbf{g})}\;\delta\mathbf{g}. \tag{48}$$

The expression (48) *is equivalent to* (45)*; only the real quantities indicated by an underbar _ are replaced by their complex-valued quantities.*

The computation of the gradient of J via the adjoint equation approach is more subtle. Formally applying the adjoint method (e.g., [33, *p.* 59]*), one might think of defining*

$$\mathbf{p}^T = -D|\mathbf{r}^*\mathbf{u}(\mathbf{g})|\;\mathbf{r}^*\mathbf{A}(\mathbf{g})^{-1} \tag{49}$$

and then writing

$$DJ(\mathbf{g})\,\delta\mathbf{g} = \mathbf{p}^T D_{\mathbf{g}}(\mathbf{A}(\mathbf{g})\mathbf{u})|_{\mathbf{u}=\mathbf{u}(\mathbf{g})}\;\delta\mathbf{g} = \Big(\big(D_{\mathbf{g}}(\mathbf{A}(\mathbf{g})\mathbf{u})|_{\mathbf{u}=\mathbf{u}(\mathbf{g})}\big)^T\mathbf{p}\Big)^T\;\delta\mathbf{g}. \tag{50}$$

In (49)*, the derivative* (47) *is applied component-wise to the vector $\mathbf{r}^*\mathbf{A}(\mathbf{g})^{-1}$ and gives the real vector $\mathbf{p} \in \mathbb{R}^n$. Since $\mathbf{A}(\mathbf{g})\mathbf{u} \in \mathbb{C}^n$ it holds that $D_{\mathbf{g}}(\mathbf{A}(\mathbf{g})\mathbf{u})|_{\mathbf{u}=\mathbf{u}(\mathbf{g})} \in \mathbb{C}^{n\times m}$, which implies that $\big(D_{\mathbf{g}}(\mathbf{A}(\mathbf{g})\mathbf{u})|_{\mathbf{u}=\mathbf{u}(\mathbf{g})}\big)^T\mathbf{p} \in \mathbb{C}^m$ and $\Big(\big(D_{\mathbf{g}}(\mathbf{A}(\mathbf{g})\mathbf{u})|_{\mathbf{u}=\mathbf{u}(\mathbf{g})}\big)^T\mathbf{p}\Big)^T\;\delta\mathbf{g} \in \mathbb{C}$. Since $DJ(\mathbf{g})\,\delta\mathbf{g} \in \mathbb{R}$ the identity (50) is* not *true. The problem is that in order to evaluate $D|\mathbf{r}^*\mathbf{u}(\mathbf{g})|$ in the direction $\delta z = \mathbf{r}^*\mathbf{A}(\mathbf{g})^{-1}D_{\mathbf{g}}(\mathbf{A}(\mathbf{g})\mathbf{u})|_{\mathbf{u}=\mathbf{u}(\mathbf{g})}\;\delta\mathbf{g}$*

we need to know the real and imaginary parts of δz*, which also depend on* $D_{\mathbf{g}}(\mathbf{A}(\mathbf{g})\mathbf{u})|_{\mathbf{u}=\mathbf{u}(\mathbf{g})}$ *which does not appear in the "adjoint equation"* (49).

We define $\mathbf{p} \in \mathbb{C}^n$ *as the solution of*

$$\mathbf{A}(\mathbf{g})\mathbf{p} = \mathbf{r} \tag{51}$$

and set $\mathbf{w}^* = \mathbf{p}^* D_{\mathbf{g}}(\mathbf{A}(\mathbf{g})\mathbf{u})|_{\mathbf{u}=\mathbf{u}(\mathbf{g})} \in \mathbb{C}^{1\times m}$*. With these definitions we can write* $DJ(\mathbf{g})\,\delta\mathbf{g} = D|\mathbf{r}^*\mathbf{u}(\mathbf{g})|\ \mathbf{w}^*\delta\mathbf{g}$*. From* (47) *we find that for any real vector* $\delta\mathbf{g} \in \mathbb{R}^m$ *we have*

$$DJ(\mathbf{g})\,\delta\mathbf{g} = D|\mathbf{r}^*\mathbf{u}(\mathbf{g})|\ \left(\mathbf{w}^*\delta\mathbf{g}\right) = \left(D|\mathbf{r}^*\mathbf{u}(\mathbf{g})|\bar{\mathbf{w}}_1, \ldots, D|\mathbf{r}^*\mathbf{u}(\mathbf{g})|\bar{\mathbf{w}}_m\right)\,\delta\mathbf{g}. \tag{52}$$

Note that this associativity, $D|\mathbf{r}^*\mathbf{u}(\mathbf{g})|\ \left(\mathbf{w}^*\delta\mathbf{g}\right) = \left(D|\mathbf{r}^*\mathbf{u}(\mathbf{g})|\ \mathbf{w}^*\right)\,\delta\mathbf{g}$*, where on the right-hand side the application of* $D|\mathbf{r}^*\mathbf{u}(\mathbf{g})|$ *to the vector* $\mathbf{w}^*$ *is understood componentwise as on the right-hand side in* (52)*, is only possible because* $\delta\mathbf{g}$ *is a real vector. From* (52) *it follows immediately that*

$$\nabla J(\mathbf{g}) = \left(D|\mathbf{r}^*\mathbf{u}(\mathbf{g})|\,\bar{\mathbf{w}}_1, \ldots, D|\mathbf{r}^*\mathbf{u}(\mathbf{g})|\,\bar{\mathbf{w}}_m\right)^T. \tag{53}$$

The expression (53) *for the gradient is equivalent to* (46).

We will use the adjoint equation approach (51), (53) *to compute the gradient for the objective function* (33), (38).

Making use of the implicit function theorem, we address differentiation of $g \to U$ in Theorem 4.4, while differentiation of $U \to R$ is addressed in Proposition 4.5; differentiation of $R \to \frac{1}{2}(|\cdot| - r_k)^2$ is straightforward.

THEOREM 4.4. *Given a frequency* ω*, if* $g_0 \in \mathcal{G}_{ad}$ *satisfies the assumptions of Lemma* 3.1*, and if there are no Jones modes, then the state* $U[g;\omega]$ *is Fréchet differentiable at* g_0 *and the derivative is given by*

$$D_g U[g_0;\omega] = -\left(D_U c(g_0, U[g_0;\omega];\omega)\right)^{-1} D_g c(g_0; U[g_0;\omega];\omega).$$

Proof. We apply the implicit function theorem (see [6, Thm. 3.1.10]) to the constraint functional $c(g, U[g;\omega];\omega)$.

By Lemma 3.1 there exists an open ball $B(g_0)$ around g_0 with $B(g_0) \subset \mathcal{C} \times \mathcal{T} \subset W^2_\infty(\Omega_0) \times L^\infty(\Omega_0)$.

By Theorem 2.9, the equation $c(g_0, U;\omega) = 0 \in \mathcal{U}'$ has a unique solution $U = U[g_0;\omega]$. The constraint $c(g, U;\omega)$ is affine-linear and continuous in U. Therefore, $D_U c(g_0, U[g_0;\omega];\omega)$ exists, and furthermore, by Theorem 2.9, $(D_U c(g_0, U[g_0;\omega];\omega))^{-1}$ is continuous. By Theorems 3.2 and 3.4, the constraint $c(g, U;\omega)$ is continuously Fréchet differentiable with respect to g on $B(g_0)$. Therefore, the result follows from the implicit function theorem. ∎

Several more derivative calculations are involved in computing the objective function derivative (54).

PROPOSITION 4.5. *Setting* $r = |x^* - \phi(x)|$*, and* $\hat{r} = (x^* - \phi(x))/r$ *(note that* $x \in \Omega_0$*, while* $x^* \in \mathbb{R}^3 \setminus \phi(\Omega_0)$*), then the representation formula* (21) *becomes*

$$R(g, U;\omega) = \int_{\Omega_0} \frac{\partial G}{\partial r}\frac{\partial r}{\partial a_3}\psi(x)\sqrt{a}\,dx,$$

and its derivatives D_gR and D_UR are

$$\begin{aligned}\langle D_gR(g,U;\omega),\delta g\rangle_{\mathbb{W}'\times\mathbb{W}} &= \int_{\Omega_0}\frac{\partial G}{\partial r}\hat{r}\cdot a_3\psi(x)D_\phi\sqrt{a}\delta\phi\,dx\\ &+\int_{\Omega_0}\left(\frac{\partial^2 G}{\partial r^2}(D_\phi r)\hat{r}\cdot a_3+\frac{\partial G}{\partial r}D_\phi\hat{r}\cdot a_3+\frac{\partial G}{\partial r}\hat{r}\cdot D_\phi a_3\right)\delta\phi\psi(x)\sqrt{a}\,dx\\ \langle D_UR(g,U;\omega),\delta U\rangle_{\mathcal{U}'\times\mathcal{U}} &= \int_{\Omega_0}\frac{\partial G}{\partial r}\hat{r}\cdot a_3\delta\psi(x)\sqrt{a}\,dx.\end{aligned}$$

Proof. The proof is analogous to that of Theorem 3.4 and has been omitted. ∎

Recall the real derivative (47) of the modulus function $|\cdot|:\mathbb{C}\to\mathbb{R}$ at a point $z=x+iy\in\mathbb{C}\setminus\{0\}$, in a direction $\delta z=\delta x+i\delta y$, and recall the definition (32) of the functional j_k. Under the assumptions of Theorem 4.4 and Proposition 4.5 and assuming $R(g,U[g;\omega_k];\omega_k)\neq 0$, $k=1,\dots,N_\omega$, the Fréchet derivative of J at a point $g\in\mathcal{G}$ in a direction $\delta g\in\mathbb{W}:=W_p^3(\Omega_0)^3\times W_p^1(\Omega_0)$ is given by

$$\begin{aligned}&\langle DJ(g),\delta g\rangle_{\mathbb{W}'\times\mathbb{W}}\\ &=\sum_{k=1}^{N_\omega}\alpha_k\left(D_gj_k(g,U[g;\omega_k];\omega_k)\delta g+D_Uj_k(g,U[g;\omega_k];\omega_k)\left(D_gU[g;\omega_k]\right)\right)\delta g,\end{aligned}\tag{54}$$

where D_gj_k and D_Uj_k are

$$\begin{aligned}D_gj_k(g,U[g;\omega_k];\omega_k) &= \left(|R(g,U[g;\omega_k];\omega_k)|-r_k\right)\\ &\quad\times D|R(g,U[g;\omega_k];\omega_k)|D_gR(g,U[g;\omega_k];\omega_k),\\ D_Uj_k(g,U[g;\omega_k];\omega_k) &= \left(|R(g,U[g;\omega_k];\omega_k)|-r_k\right)\\ &\quad\times D|R(g,U[g;\omega_k];\omega_k)|D_UR(g,U[g;\omega_k];\omega_k).\end{aligned}$$

In order to evaluate (54) using the above calculations, we must handle the term

$$\langle D_Uj_k(g,U[g;\omega_k];\omega_k)\left(D_gU[g;\omega_k]\right),\delta g\rangle_{\mathbb{W}'\times\mathbb{W}}.\tag{55}$$

Invoking Theorem 4.4, the state derivative $D_gU[g;\omega_k]$ can be replaced by

$$D_gU[g;\omega_k]=-D_Uc(g,U[g;\omega_k];\omega_k)^{-1}D_gc(g;U[g;\omega_k];\omega_k),$$

whence (55) becomes

$$\begin{aligned}&\langle -D_Uj_k(g,U[g;\omega_k];\omega_k)D_Uc(g,U[g;\omega_k];\omega_k)^{-1},D_gc(g;U[g;\omega_k];\omega_k)\delta g\rangle_{\mathcal{U}\times\mathcal{U}'}\\ &\quad=\langle -D_Uj_k(g,U[g;\omega_k];\omega_k),D_Uc(g,U[g;\omega_k];\omega_k)^{-1}D_gc(g;U[g;\omega_k];\omega_k)\delta g\rangle_{\mathcal{U}'\times\mathcal{U}}\\ &\quad=\langle -D_Uc(g,U[g;\omega_k];\omega_k)^{-*}D_Uj_k(g,U[g;\omega_k];\omega_k),D_gc(g;U[g;\omega_k];\omega_k)\delta g\rangle_{\mathcal{U}\times\mathcal{U}'}.\end{aligned}\tag{56}$$

The so-called sensitivity approach would be to evaluate (56) for each desired direction δg, but this is extremely expensive, as it requires the solution of (30) for every δg in order to apply $D_Uc(g,U[g;\omega_k];\omega_k)^{-1}$.

As motivated by Example 4.3 we use the adjoint equations

$$D_Uc(g,U[g;\omega_k];\omega_k)^*P_k=-D_UR(g,U[g;\omega_k];\omega_k).\tag{57}$$

Given that c is affine-linear in U, and writing $P = (\xi, w)$, $V = (\eta, y)$, the adjoint operator $D_U c^*$ takes the form (cf. (30))

$$\begin{aligned}\langle D_U c(g,U;\omega)^* P, V\rangle_{\mathcal{U}'\times\mathcal{U}} &= K(\eta,y;\overline{\xi},\overline{w}) - \omega^2 M(\eta,y;\overline{\xi},\overline{w}) \\ &\quad - \int_{\Omega_0} (f\cdot\overline{w} - i\omega\rho_0\psi\overline{w}\cdot n)\sqrt{a}\,dx \\ &\quad + \langle D(\phi)\psi, \overline{\varrho}\rangle_{H^{-1/2}(\phi(\Omega_0))\times\widetilde{H}^{1/2}(\phi(\Omega_0))} \\ &\quad - \int_{\Omega_0} i\omega y(x)\cdot a_3(x)\,\overline{\varrho}(x)\sqrt{a}\,dx.\end{aligned}$$

The objective function derivative (54) is then computed after N_ω state and N_ω adjoint solves via (cf. (56))

$$\begin{aligned}\langle DJ(g), \delta g\rangle_{\mathbb{W}'\times\mathbb{W}} &= \sum_{k=1}^{N_\omega} \alpha_k(|R(g,U[g;\omega_k];\omega_k)| - r_k)D|\cdot| \\ &\quad \times (\langle D_g R(g,U[g;\omega_k];\omega_k), \delta g\rangle_{\mathbb{W}'\times\mathbb{W}} \\ &\quad + \langle D_g c(g,U[g;\omega_k];\omega_k)\delta g, P_k\rangle_{\mathcal{U}'\times\mathcal{U}}).\end{aligned} \tag{58}$$

While numerical solution of the adjoint equation (57) is quite straightforward given a numerical scheme for solving the state equation (30), implementation of a numerical scheme for application of the adjoint state in (58) is quite involved due to presence of the term $D_g c$, which is a Fréchet derivative of the shell and boundary integral operators. If these are discretized respectively with finite and boundary element methods, then the discretization of $D_g c$ is a very large, sparse tensor. The tensor need not be stored, but rather must be applied to the state U and adjoint state P. In the case of shell finite elements, this application is tedious, but straightforward. For boundary element methods, where even computing all of the tensor entries is impractically expensive, we suggest the tensor approximation method of [4], which extends the adaptive cross approximation [59] for application of matrix-vector products.

5. Numerical example. To illustrate the applicability of our theory, we apply it to the optimization of joined shells shown on the left in Figure 2 below. Our reference domain is a box with a circular hole at the top and walls of constant thickness. We use the coupling conditions for Naghdi shells [31], which are derived from the junction conditions in [7, 8, 9, 23, 24, 40] for several typically simpler problems (such as plates

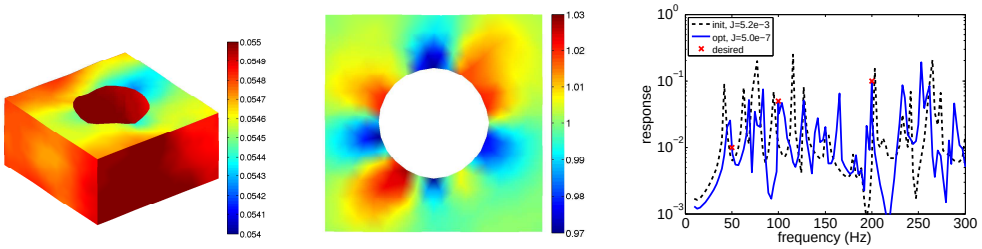

FIG. 2. *The initial shape was a box with flat faces and uniform thickness of* 0.05. *Left plot: The optimized shape. Color indicates the shell thickness. Center plot: The top face. Color indicates shell height. Right plot: The transfer functions corresponding to the initial shape and the optimized shape, as well as the* $N_\omega = 3$ *frequencies with corresponding desired values* r_k *for the transfer function (×).*

or Koiter shells). We sketch the main components of our numerical approach and refer to [31] for additional details.

We discretize (28) using finite element methods with carefully chosen element spaces. It is well known that naïve finite element approximations of the Naghdi shell equations exhibit a highly undesirable locking behavior. Therefore we use MITC finite elements. See [15, 16]. For plates, convergence analysis of MITC elements is surveyed in [26]. Although the MITC theory for shells is less developed, numerical experiments such as those reported in [3, 5, 42] show approximation properties similar to those known for plates. See also [16].

We enforce the coupling conditions for the joined shells by introducing Lagrange multipliers. For example, for two joined shells the finite element system is given by

(59)
$$\begin{pmatrix} \mathbf{K}_1(\mathbf{g}) - \omega^2\mathbf{M}_1(\mathbf{g}) & \mathbf{0} & \mathbf{C}_1(\mathbf{g})^T & i\omega\rho_0\mathbf{N}_1(\mathbf{g})^T \\ \mathbf{0} & \mathbf{K}_2(\mathbf{g}) - \omega^2\mathbf{M}_2(\mathbf{g}) & \mathbf{C}_2(\mathbf{g})^T & i\omega\rho_0\mathbf{N}_2(\mathbf{g})^T \\ \mathbf{C}_1(\mathbf{g}) & \mathbf{C}_2(\mathbf{g}) & \mathbf{0} & \mathbf{0} \\ -i\omega\mathbf{N}_1(\mathbf{g}) & -i\omega\mathbf{N}_2(\mathbf{g}) & 0 & \mathbf{D}(\mathbf{g},\omega) \end{pmatrix} \begin{pmatrix} \mathbf{S}_1 \\ \mathbf{S}_2 \\ \boldsymbol{\lambda} \\ \boldsymbol{\psi} \end{pmatrix} = \begin{pmatrix} \mathbf{F}_1(\mathbf{g}) \\ \mathbf{F}_2(\mathbf{g}) \\ \mathbf{0} \\ \mathbf{0} \end{pmatrix}.$$

The equation $\mathbf{C}_1(\mathbf{g})\mathbf{S}_1 + \mathbf{C}_2(\mathbf{g})\mathbf{S}_2 = \mathbf{0}$ is the conditions for joining two shells and $\boldsymbol{\lambda}$ is the corresponding vector of Lagrange multipliers. The matrices $\mathbf{K}_j(\mathbf{g}), \mathbf{M}_j(\mathbf{g})$, $j = 1, 2$ arise from the discretization of (9) and (11) for the two shells. These matrices are large, but are sparse and symmetric. The (sparse) matrices $\mathbf{N}_1(\mathbf{g}), \mathbf{N}_2(\mathbf{g})$ represent the coupling terms between the BEM and shell equations in the weak formulation (28). The last row of (59) is a discretization of (28b), with $\mathbf{D}(\mathbf{g}, \omega)$ corresponding to (23), except that we now make its dependence on the frequency explicit. In the following we write the system arising from the discretization of the coupled structural-acoustic system in the short form

$$\mathbf{c}(\mathbf{g}, \omega)\mathbf{U} = \mathbf{F}(\mathbf{g}). \tag{60}$$

In the case of two coupled shells, (60) represents the system (59).

Our objective function is a discretization of (31)–(33). A discretization of a coupled structural-acoustic optimization problem has the form

$$\text{minimize } J(\mathbf{U}_1(\mathbf{g}), \ldots, \mathbf{U}_{N_\omega}(\mathbf{g}), \mathbf{g}), \tag{61a}$$

$$\text{subject to } \mathbf{A}\mathbf{g} \le \mathbf{b}, \tag{61b}$$

$\mathbf{U}_k$ solves $\mathbf{c}(\mathbf{g}, \omega_k)\mathbf{U}_k = \mathbf{F}_k(\mathbf{g})$, $k = 1, \ldots, N_\omega$, and where the inequality constraints $\mathbf{A}\mathbf{g} \le \mathbf{b}$ represent explicit bounds on the discretized chart and thickness function originating from (14), (35). The bound M on the discretized states (39b) was chosen large enough to be never active in our example and therefore the bound constraint on the discretized states has been omitted in (61).

Figure 2 shows the result of our computation for a small version of a coupled structural-acoustic optimization problem (61). The initial geometry consists of six shells (initially they are flat, i.e., are plates) of uniform thickness joined to form the box with a circular hole in the top, see the left plot of Figure 2), and generated using Gmsh [29]. The optimization variables are the thickness functions of the shells as well as their midsurface charts. The objective function measures the mismatch of the response $R(x^*)$ at an external point x^* from a desired response (× in Figure 2) for $N_\omega = 3$ frequencies. We use weights $\alpha_1 = \alpha_2 = \alpha_3 = 1$.

Even in this simple example, we already have nearly 5,000 shape parameters $\mathbf{g}$ and 35,000 inequality constraints (61b) Moreover, for each frequency ω_k we have around 12,000 state variables corresponding to the shell displacements (θ_k, z_k) and the jump ψ_k in the acoustic potential.

6. Conclusions. We have developed a framework for shape optimization of shell structure acoustics based on a mathematical model coupling Naghdi shell equations with screen boundary integral equations (section 2.3), including the necessary tools for the application of gradient-based optimization algorithms: existence of optimal solutions, and efficient calculation of the objective function gradient based on adjoint equations.

As discussed in section 4.2, a significant challenge in the implementation is the application of the Fréchet derivative of the boundary integral operator $D_\phi D$ (29), a component of $D_g c$, which is needed for the gradient computation in (58). Efficient numerical approximation of $D_\phi D$ can be performed using the method in [4]. This approach avoids additional analytical work otherwise needed to characterize the shape derivative of the state for the coupled problem, and considerably simplifies the implementation. The form of (30) suggests discretization using shell finite elements and Galerkin boundary elements, and this is the approach used in the numerical examples presented in [31] and section 5, albeit without the tensor approximation method of [4]. Future work will include combining these techniques so as to be able to solve truly large-scale optimization problems.

Acknowledgments. We thank the referees for their careful reading of the paper, which have led to improvements in the presentation.

REFERENCES

[1] H. Antil, S. Hardesty, and M. Heinkenschloss, *Supplementary materials: Shape optimization of shell structure acoustics*, Department of Computational and Applied Math., Rice University, Houston, Texas, 2016, http://www.caam.rice.edu/~heinken/papers/HAntil_SHardesty_MHeinkenschloss_2016b.pdf.

[2] V. Arnăutu, J. Sprekels, and D. Tiba, *Optimization problems for curved mechanical structures*, SIAM J. Control Optim., 44 (2005), pp. 743–775 (electronic).

[3] K. J. Bathe, A. Iosilevich, and D. Chapelle, *An evaluation of the MITC shell elements*, Comput. Struct., 75 (2000), pp. 1–30.

[4] M. Bebendorf and S. Hardesty, *Adaptive cross approximation of tensors arising in the discretization of boundary integral operator shape derivatives*, Eng. Anal. Bound. Elem., 37 (2013), pp. 60–67.

[5] L. Beirão da Veiga, D. Chapelle, and I. P. Suarez, *Towards improving the MITC6 triangular shell element*, Comput. Struct., 85 (2007), pp. 1589–1610.

[6] M. Berger, *Nonlinearity and Functional Analysis*, Academic Press, Boston, 1977.

[7] M. Bernadou and A. Cubier, *Numerical analysis of junctions between thin shells. I. Continuous problems*, Comput. Methods Appl. Mech. Eng., 161 (1998), pp. 349–363.

[8] M. Bernadou and A. Cubier, *Numerical analysis of junctions between thin shells. II. Approximation by finite element methods*, Comput. Methods Appl. Mech. Eng., 161 (1998), pp. 365–387.

[9] M. Bernadou, S. Fayolle, and F. Léné, *Numerical analysis of junctions between plates*, Comput. Methods Appl. Mech. Eng., 74 (1989), pp. 307–326.

[10] J. Bielak, R. C. MacCamy, and X. Zeng, *Stable coupling method for interface scattering problems by combined integral equations and finite elements*, J. Comput. Phys., 119 (1995), pp. 374–384.

[11] K.-U. Bletzinger, M. Bischoff, and E. Ramm, *A unified approach for shear-locking free triangular and rectangular shell finite elements*, Comput. Struct., 75 (2000), pp. 321–334.

[12] A. Blouza, *Existence et unicité pour le modèle de Nagdhi pour une coque peu régulière*, C. R. Acad. Sci. Paris, Sér. I, Math., 324 (1997), pp. 839–844.

[13] A. Blouza and H. Le Dret, *Existence and uniqueness for the linear Koiter model for shells with little regularity*, Quart. Appl. Math., 57 (1999), pp. 317–337.
[14] A. Blouza and H. Le Dret, *Nagdhi's shell model: Existence, uniqueness and continuous dependence on the midsurface*, J. Elasticity, 64 (2001), pp. 199–216.
[15] D. Braess, *Finite Elements. Theory, Fast Solvers, and Applications in Solid Mechanics*, Cambridge University Press, Cambridge, 1997.
[16] D. Chapelle and K. J. Bathe, *The Finite Element Analysis of Shells—Fundamentals*, 2nd ed., Computational Fluid and Solid Mechanics, Springer-Verlag, Berlin, 2011.
[17] S. T. Christensen and N. Olhoff, *Shape optimization of a loudspeaker diaphragm with respect to sound directivity properties*, Control Cybern., 27 (1998), pp. 177–198.
[18] S. T. Christensen, S. V. Sorokin, and N. Olhoff, *On analysis and optimization in structural acoustics. Part II: Exemplifications for axisymmetric structures*, Struct. Optim., 16 (1998), pp. 96–107.
[19] P. G. Ciarlet, *An introduction to differential geometry with application to elasticity*, J. Elasticity, 78/79 (2005).
[20] M. Costabel, *Boundary integral operators on Lipschitz domains: Elementary results*, SIAM J. Math. Anal., 19 (1988), pp. 613–626.
[21] M. C. Delfour, *Characterization of the space of solutions of the membrane shell equation for arbitrary $C^{1,1}$ midsurfaces*, Control Cybern., 28 (1999), pp. 481–501. Special issue: Recent advances in control of PDEs.
[22] M. C. Delfour, *Representations of hypersurfaces and minimal smoothness of the midsurface in the theory of shells*, Control Cybern., 37 (2008), pp. 879–911.
[23] H. L. Dret, *Folded plates revisited*, Comput. Mech., 5 (1989), pp. 345–365.
[24] H. L. Dret, *Modeling of a folded plate*, Comput. Mech., 5 (1990), pp. 401–416.
[25] H. L. Dret, *Well-posedness for Koiter and Naghdi shells with a G_1-midsurface*, Anal. Appl., Singap., 2 (2004), pp. 365–388.
[26] R. S. Falk, *Finite elements for the Reissner-Mindlin plate*, in Mixed Finite Elements, Compatibility Conditions, and Applications, Lectures given at the C.I.M.E. Summer School held in Cetraro, Italy, June 26–July 1, 2006, Lecture Notes in Mathematics 1939, Springer-Verlag, Berlin, 2008, pp. 195–232.
[27] M. Fischer and L. Gaul, *Fast BEM-FEM mortar coupling for acoustic-structure interaction*, Int. J. Numer. Methods Eng., 62 (2005), pp. 1677–1690.
[28] D. Fritze, S. Marburg, and H.-J. Hardtke, *FEM–BEM-coupling and structural-acoustic sensitivity analysis for shell geometries*, Comput. Struct., 83 (2005), pp. 143–154.
[29] C. Geuzaine and J.-F. Remacle, *Gmsh: A 3-D finite element mesh generator with built-in pre- and post-processing facilities*, Int. J. Numer. Methods Eng., 79 (2009), pp. 1309–1331.
[30] C. Gough, *The violin: Chladni patterns, plates, shells and sounds*, Eur. Phys. J., Spec. Top., 145 (2007), pp. 77–101.
[31] S. Hardesty, *Optimization of Shell Structure Acoustics*, Ph.D. thesis, Department of Computational and Applied Mathematics, Rice University, Houston, TX, 2010. Available as CAAM TR10–16 from http://www.caam.rice.edu/tech_reports.html.
[32] T. Hargé, *Eigenfunction for an elastic body*, C. R. Acad. Sci. Paris, Ser. I, Math., 311 (1990), pp. 857–859.
[33] M. Hinze, R. Pinnau, M. Ulbrich, and S. Ulbrich, *Optimization with PDE Constraints*, Mathematical Modelling, Theory and Applications 23, Springer-Verlag, Heidelberg, 2009.
[34] I. Hlaváček and J. Lovíšek, *Optimal design of an elastic plate with unilateral elastic foundation and rigid supports, using the Reissner-Mindlin plate model. I. Continuous problems*, Z. Angew. Math. Mech., 77 (1997), pp. 377–385.
[35] G. C. Hsiao and W. L. Wendland, *Boundary Integral Equations*, Springer-Verlag, Berlin, 2008.
[36] L. Jentsch and D. Natroshvili, *Interaction between thermoelastic and scalar oscillation fields*, Integral Equations Oper. Theory, 28 (1997), pp. 261–288.
[37] L. Jentsch and D. Natroshvili, *Non-local approach in mathematical problems of fluid-structure interaction*, Math. Methods Appl. Sci., 22 (1999), pp. 13–42.
[38] A. M. Khludnev and J. Sokolowski, *Modelling and Control in Solid Mechanics*, International Series of Numerical Mathematics 122, Birkhäuser Verlag, Basel, 1997.
[39] N. H. Kim and J. Dong, *Shape sensitivity analysis of sequential structural-acoustic problems using FEM and BEM*, J. Sound Vib., 290 (2006), pp. 192–208.
[40] J. E. Lagnese and G. Leugering, *Modelling of dynamic networks of thin elastic plates*, Math. Methods Appl. Sci., 16 (1993), pp. 379–407.
[41] J. Lee and S. Wang, *Shape design sensitivity analysis for the radiated noise from the thin-body*, J. Sound Vib., 261 (2003), pp. 895–910.

[42] P.-S. Lee and K. J. Bathe, *Development of MITC isotropic triangular shell finite elements*, Comput. Struct., 82 (2004), pp. 945–962.
[43] C. J. Luke and P. A. Martin, *Fluid-solid interaction: acoustic scattering by a smooth elastic obstacle*, SIAM J. Appl. Math., 55 (1995), pp. 904–922.
[44] S. Marburg, *Efficient optimization of a noise transfer function by modification of a shell structure geometry – Part I: Theory*, Struct. Multidiscip. Optim., 24 (2002), pp. 51–59.
[45] S. Marburg, *A general concept for design modification of shell meshes in structural-acoustic optimization: Part I: Formulation of the concept*, Finite Elem. Anal. Des., 38 (2002), pp. 725–735.
[46] S. Marburg and H.-J. Hardtke, *Efficient optimization of a noise transfer function by modification of a shell structure geometry – Part II: Application to a vehicle dashboard*, Struct. Multidiscip. Optim., 24 (2002), pp. 60–71.
[47] S. Marburg and H.-J. Hardtke, *A general concept for design modification of shell meshes in structural-acoustic optimization: Part II: Application to a floor panel in sedan interior noise problems*, Finite Elem. Anal. Des., 38 (2002), pp. 737–754.
[48] J. B. Mariem and M. A. Hamdi, *A new boundary finite element method for fluid-structure interaction problems*, Int. J. Numer. Methods Eng., 24 (1987), pp. 1251–1267.
[49] R. Martinez, *The thin-shape breakdown (TSB) of the Helmholtz integral equation*, J. Acoust. Soc. Amer., 90 (1991), pp. 2728–2738.
[50] W. McLean, *Strongly Elliptic Systems and Boundary Integral Equations*, Cambridge University Press, Cambridge, 2000.
[51] R. Potthast, *Fréchet differentiability of boundary integral operators in inverse acoustic scattering*, Inverse Probl., 10 (1994), pp. 431–447.
[52] R. Potthast, *Fréchet differentiability of the solution to the acoustic Neumann scattering problem with respect to the domain*, J. Inverse Ill-Posed Probl., 4 (1996), pp. 67–84.
[53] R. Remmert, *Theory of Complex Functions*, Graduate Texts in Mathematics 122, Springer-Verlag, New York, 1991. Translated from the second German edition by Robert B. Burckel, Readings in Mathematics.
[54] S. Sauter and C. Schwab, *Boundary Element Methods*, Springer Series in Computational Mathematics 39, Springer-Verlag, New York, 2011.
[55] J. Sokołowski, *Displacement derivatives in shape optimization of thin shells*, in Optimization Methods in Partial Differential Equations, Proceedings of the AMS-SIAM Joint Summer Research Conference held at Mount Holyoke College, June 16–20, 1996, S. Cox and I. Lasiecka, eds., Contemporary Mathematics, 209, AMS, Providence, RI, 1997, pp. 247–266.
[56] J. Sokołowski and J.-P. Zolésio, *Introduction to Shape Optimization: Shape Sensitivity Analysis*, Springer Series in Computational Mathematics 16, Springer-Verlag, Berlin, 1992.
[57] J. Sprekels and D. Tiba, *An analytic approach to a generalized Naghdi shell model*, Adv. Math. Sci. Appl., 12 (2002), pp. 175–190.
[58] E. P. Stephan, *Boundary integral equations for screen problems in* $\mathbf{R}^3$, Integral Equations Oper. Theory, 10 (1987), pp. 236–257.
[59] M. Stolper, *Computing and compression of the boundary element matrices for the Helmholtz equation*, J. Numer. Math., 12 (2004), pp. 55–75.
[60] J. Woodhouse, *The acoustics of the violin: A review*, Rep. Prog. Phys., 77 (2014), p. 115901.
[61] G. H. Yoon, J. S. Jensen, and O. Sigmund, *Topology optimization of acoustic-structure interaction problems using a mixed finite element formulation*, Int. J. Numer. Methods Eng., 70 (2007), pp. 1049–1075.